Transport of nitrogen oxides and nitric acid pollutants over South Africa and air pollution in Cape Town

by

Adefolake Mayokun Ojumu

submitted in accordance with the requirements for
the degree of

Master of Science

In the subject of

Environmental Science

at the

University of South Africa

Supervisor: Dr Babatunde Joseph Abiodun

September 2013

Abstract

The deteriorating air quality in Cape Town (CT) is a threat to the social and economic development of the city. Although previous studies have shown that most of the pollutants are emitted in the city, it is not clear how the transport of pollutants from neighbouring cities may contribute to the pollution. This thesis studies the transport of atmospheric nitrogen oxides (NO_x) and nitric acid (HNO_3) pollutants over South Africa and examines the role of pollutant transport from the Mpumalanga Highveld on pollution in CT.

The study analysed observation data (2001 - 2008) from the CT air quality network and from regional climate model simulation (2001 - 2004) over South Africa. The model simulations account for the influences of complex topography, atmospheric conditions, and atmospheric chemistry on transport of the pollutants over South Africa. Flux budget analysis was used to examine whether the city is a net source or sink for NO_x and HNO_3.

The results show that north-easterly flow transports pollutants (NO_x and HNO_3) at low level (i.e., surface to 850 hPa) from the Mpumalanga Highveld towards CT. In April, a tongue of high concentration of HNO_3 extends from the Mpumalanga Highveld to CT, along the southern coast. The flux budget analysis shows that CT can be a net sink for NO_x and HNO_3 during extreme pollution events. The study infers that, apart from the local emission of the pollutants in CT, the accumulation of pollutants transported from other areas may contribute to pollution in the city.

Keywords: Air Pollution, Atmospheric pollution, Flux budget analysis, Extreme pollution events, Pollutants transport, Pollutants concentration, Atmospheric-chemistry model, Eulerian pollution model, RegCM, Diurnal variation

Declaration

- I know that plagiarism is wrong. Plagiarism is to use another's work and pretend it is one's own.
- This submission is my own work.
- I have not allowed, and will not allow, anyone to copy my work with the intention of passing it off as their own work.
- I acknowledge that copying someone else's assignment or essay, or part of it, is wrong, and declare that this is my own work.

First Name and Surname
Adefolake Mayokun Ojumu

Student Number:
46285318

12/09/2013

Signature

Date

Acknowledgements

I wish to thank:

- My God, who has helped me to complete this research work.
- My supervisor, Dr. Babatunde Joseph Abiodun, for the untiring guidance and courage given to me throughout the research, despite his busy schedules.
- My lovely parents, for allowing me to embark on this seemingly long course of study.
- My loving husband, Prof Tunde Ojumu, for his financial support on the thesis.
- My precious children, Victor, Favour and Emmanuel, for their prayers towards the success of this project.
- My colleagues, Samantha Jenner, Anu Olanrewaju, and Kehinde Kenneth, for their constructive advice and technical support towards the completion of this work.

Dedication

I dedicate this work to God Almighty, my creator, who has always been the driving force behind all my achievements.

Contents

List of Figures

List of Tables

Glossary

Acronyms	Definition
BATS	Biosphere-Atmosphere Transfer Scheme
CCM3	Climate community model, version 3
CCSM	Community Climate System Model
CEM	Common Land Model
CLM	Continuous Emissions Monitor
CT	Cape Town
EPA	Environmental Protection Agency
HNO_3	Nitric acid
ICTP	International Centre for Theoretical Physics
NHO_3	Nitric Acid
NCAR	National Centre of Atmospheric Research
NO	Nitrogen oxide
NO_2	Nitrogen dioxide
NO_X	Oxides of Nitrogen
O_3	Ozone
PM	Particulate Matter
RegCM	Regional Climate Model
SAWS	South African Weather Service
SO_2	Sulphur dioxide
VOC	Volatile Organic Compound
WHO	World Health Organisation

Chapter One: Introduction

1.0 Introduction

Cape Town is one of the many cities in the world that has problems with air pollution. Air pollution occurs when the pollutant concentrations (gases or dust) in the air reach harmful levels; that is, the concentration of pollutants reaches an amount that can harm human health (and comfort) or damage the environment (plants and materials). Most air pollution is caused by anthropogenic activities that release pollutants into the atmosphere, especially in industrial areas and urban centres. Since the effect of air pollution on humans and the environment is always undesirable (Seinfeld & Pandis 2006), there is a keen interest to identify its cause over cities and address sources using different rules and regulations. For instance, in South Africa, different laws and policies are in place (at national and local authority levels) to combat air pollution in the country (Kalognomou 2009); however, for these laws and policy to be effective there is a need to identify, not only the local sources of pollutants within a city, but also the remote sources of pollutants as air pollution problems in a city may be caused by pollutants emitted outside the city.

1.1 Problems associated with air pollution

Air pollution in the cities is linked to many problems. It can reduce atmospheric visibility, corrode buildings, decrease crop yields, and alter ecosystems (Jury et al., 1990:4 Tegen et al 1990:4; Tamm 1976:236). More importantly, air pollution can damage human health. A number of epidemiological diseases are attributed to human exposures to ambient air pollution (The World Health Organisation (WHO). Even an exposure to low concentrations of particulate matter (PM) can lead to premature death in the elderly and people with a pre-existing heart disease (Fitzpatrick, 2006). Cardiopulmonary disease, lung cancer and acute respiratory infections in children are caused by exposure to a high concentration of PM in the atmosphere (Norman et al 2007:783). Children's exposure to high levels of lead are linked to a low intelligence quotient (IQ) and slow development (WHO). In addition, many studies have linked high concentrations of oxides of nitrogen (NO_x), sulphur dioxide (SO_2) and volatile organic compounds (VOCs) to various ill-health effects (Atkins 2010:23). Table (1.1) gives a summary of pollutants, their sources and their impact on health.

Table 1.1: Impact of air pollutants on health.

Pollutants	Sources	Health effects
Ozone (O_3)	Action of sunlight on NO_2 i.e., photolysis	• Cause asthma, bronchitis, irritation to the eyes and mucous membranes • Causes headache, nose and throat irritation
Aerosols	Particles or conversion of certain gases in the atmosphere	• Inhibits visibility and increases human mortality
Lead (Pb)	Transportation and industry	• Reduces birth weight and lowers IQ. Cause neurocognitive and neuromotor impairment
Carbon	Burning of fossil fuel. Incomplete combustion in motor vehicles	• Reduces ability of the circulatory system to transport oxygen • Impairs of performance on tasks requiring attention. • Aggravates cardiovascular diseases.
Suspended particles	Burning of fossil fuels	• Damages to lungs tissues causing respiratory disease.
Sulphur dioxide	Burning of fossil fuels, untarred roads, mining dusts and agriculture	• Causes constriction of the airways in people with asthma • Causes a condition similar to bronchitis. • Increases the risk of acute respiratory disease.
Nitrogen	Burning of fossil fuels, especially motor vehicles	• Can irritate the lungs and aggravate the condition of people suffering from asthma and chronic bronchitis
Hydrocarbons	Vehicles and industrial processes.	• Can cause some defects in babies during pregnancy or cancer
Heavy metals	Industry and motor vehicles	• Causes cancer, defects in babies during pregnancy

Source: Greater Johannesburg Metropolitan Council (2000).

1.2 The chemical and environmental impacts of NO_x and HNO_3

Mono-nitrogen oxides (NO_x) and nitric acid (HNO_3) can have severe impacts on human health and the environment. NO_x concentration in the atmosphere is essentially the total concentration of nitric oxide (NO) and nitrogen dioxide (NO_2), while the acid derivate, HNO_3, is an oxidative product of NO_x as shown in equations. (1.1) - (1.4).

$$NO + O_3 \rightarrow NO_2 + O_2 \quad (1.1)$$

$$NO_2 + O \rightarrow NO + O_2 \quad (1.2)$$

$$4\ NO + 3\ O_2 + 2\ H_2O \rightarrow 4\ HNO_3 \quad (1.3)$$

$$2\ NO_2 + H_2O \rightarrow HNO_2 + HNO_3 \quad (1.4)$$

The conversion of NO to NO_2 depends on the ozone availability, sunshine and temperature, and HNO_3 is produced from dissolution of NO_2 in moisture (Seinfeld & Pandis 2006). Since NO is a greenhouse gas, atmospheric NO may contribute to global warming, which threatens both environment and human health. The reaction of NO_x and sulphur dioxide in the presence of moisture produces acid rain, which corrodes cars, buildings and historical monuments and makes streams and lakes acidic which render them uninhabitable for fish. The reaction of NO_x and ammonia with other substances generates particles and nitric acid. These particles have a negative impact on the human respiratory system by damaging lung tissue and causing premature death. Small particles, in particular, can penetrate deeply into sensitive parts of the human lung and cause respiratory diseases such as emphysema and bronchitis which can aggravate an existing heart disease. Nitric acid corrodes and degrades metals (Dean 1990). Excess nitrate is harmful to ecosystems because it can lead to "eutrophication", which deteriorates water quality and kills fish; however, the complexity of nutrient cycling in ecosystems often takes decades to become apparent due to the long-term impact of nitric acid (Fields 2004). Reaction of NO_x with VOCs in the presence of heat and sunlight produces smog (ground-level ozone). Smog and ozone are well known causes of nose and throat irritation and eventual death. Cape Town is usually covered with smog (called "brown haze") in winter. Several studies (Wicking-Baird et al 1997:iii) have linked the brown haze to unpleasant odours, health effects and visibility impairment in Cape Town. Jacobson (2002:99) showed that the reddish brown colour in smog can be attributed to the presence of NO_2, absorption in the ultraviolent and visible by nitrated aromatics and polycyclic aromatic hydrocarbons in aerosol particles, with an occasional and small enhancement by suspended soil and dust. Two potential causes of brown-yellow smog have been identified as light absorption by gaseous NO_2 and wavelength dependent light scattering by aerosols. The angle between the observer's line of sight and the sun plays an important role in the coloration of the smog layer and also determines the relative importance of NO_2 and aerosol (Husar & White 1976).

1.3 Air pollution in Cape Town

Air pollution problems remain a threat to the socio-economic developments in Cape Town. In 2003, the concentration of pollutants in the city exceeded the internationally accepted guidelines for more than half of the year. In 2006 and 2007, air pollution

throughout Cape Town exceeded the WHO air quality guidelines for a period of more than 162 days (allAfrica 2008). Poor visibility (Fig. 1.1) due to air pollution is worst in the centre of Cape Town where the level of human activities is higher than that of the rural areas (CCT, 2005). Levels of pollutants were also reportedly high in the industrial areas and in the highly populated areas of the city (White et al 2009).

Figure 1.1: Poor visibility induced by air pollution in Cape Town
Source: The City of Cape Town (CCT), 2005.

Some of these harmful pollutants have their sources (emissions) in the growth of human activities (inter alia, industries, traffic, agriculture), which sustain the economy of the city (Kalognomou 2009:79; CCT 2005:10-17). While a further increase in these activities could worsen the air pollution problem; an unplanned decrease in the activities could also impede the economic development. Hence, there is need for a good balance between reducing the rate of emissions and improving the economy.

One way to reduce air pollution problems is to keep the concentrations of these air pollutants below the standard level prescribed by the Environmental Protection Agency

(Maynard & Maynard 2002:5561; Zunckel et al 2004a:6140); however, despite the recent reduction in emissions from a petroleum refinery suspected to be the major pollution source in the city, the air quality in CT has not improved. The reason could be that the contributions from either other local sources or from neighbouring cities are higher than that of the refinery. Nevertheless, a good knowledge of the relative contribution of emission sources from outside Cape Town is needed to efficiently reduce pollution in the city. This requires maps of pollutant concentrations, not only over the city, but also over the entire South Africa to help assess the contribution of pollutants transported from neighbouring cities.

1.4 The roles of Environmental Factors on Urban Air Quality.

Although, the amount and kind of pollutants released into the air play a major role in determining the degree of urban pollution, environmental factors are involved. The environmental factors include: topography (mountains, valleys, etc); and weather (wind, temperature, air turbulence, air pressure, rainfall and cloud cover). Poor air quality can result from a combination of factors. Therefore, urban air quality is affected by how air behaves as a result of the interaction of topography and weather, and by the emission sources. Air pollutants mix and disperse quickly in a large airshed because the air flow is not limited by topography. So the pollutants can travel and mix with the air over great distances, resulting in good air quality in the airshed. Sometimes, topography and weather combine to prevent pollutants from mixing and dispersing. In this case the pollutants become trapped within the area, resulting in poor air quality in the air shed.

Once pollutants are emitted into the air, the weather largely determines how well they disperse. Turbulence mixes pollutants into the surrounding air. For instance, during a hot summer day, the air near the surface can be much warmer than the air above (known unstable condition); this will allow the warm air to rise to great heights and this result in vigorous mixing. Wind speed also contributes to how quickly pollutants are carried away from their original source. It should be noted that strong winds don't always disperse the pollutants; they can only transport pollutants to a larger area. Sometimes the condition of the atmosphere is still very stable and this results in vigorous mixing. This occurs when the air near the surface of the earth is cooler than the air above (known as temperature inversion). Any pollutants released near the surface will be trapped and build up in the

cooler layer of air near the surface. Temperature inversions are very common in Cape Town, especially in mountain valleys. They are often formed during calm clear nights with light winds, and may persist throughout the day during the winter.

1.5 Research Questions

(i) What are the characteristics (diurnal and annual cycles) of the pollutants (NO, NO_2 and HNO_3) concentration in Cape Town?
(ii) How do the atmospheric conditions influence the diurnal and seasonal cycles of the pollutants concentrations?
(iii) How well can an atmospheric – chemistry model (for this study RegCM) simulate the characteristics of pollutants concentration in Cape Town?
(iv) What atmospheric condition favours the transport of pollutants from the Mpumalanga Highveld to Cape Town?
(v) Is Cape Town a source or sink to the pollutants?

1.6 Aim and objectives

This thesis aims to study characteristics of pollutant (NO_x and HNO_3) over Cape Town and investigate the influence of pollutants from the Mpumalanga Highveld on pollution in Cape Town.

The objectives of the study are to:

(i) examine the characteristics of NO_x and HNO_3 concentrations and atmospheric condition over Cape Town;
(ii) evaluate the capability of RegCM in simulating the atmospheric condition, NO_x and HNO_3 concentration and incorporate the chemistry simulation of pollutants over Cape Town;
(iii) study the transport of NO_x and NHO_3 over South Africa and investigate the atmospheric condition that favours the transport of the pollutants from the Mpumalanga Highveld to Cape Town;
(iv) investigate whether Cape Town is a source or sink for NO_x and NHO_3; and
(v) investigate the diurnal and seasonal circle of these pollutants.

1.7 Thesis Outline

The thesis is divided into five chapters. Chapter one provides an overview of the task done in this research. Chapter two presents a literature review on the relevant pollution studies over Cape Town. Chapter three describes the data and methodology adopted in

the thesis. This includes a brief description of Cape Town air-quality station network, the regional climate model (RegCM) with the simulation set-up, and the budget analysis. Chapter four presents and discusses the results of the study: it describes the characteristics of the meteorological and air quality over Cape Town; evaluates the model's ability to simulate the characteristics: and studies the transports of pollutants over South Africa, with emphasis on the atmospheric condition that favours the transport of pollutants from Mpumalanga Highveld to Cape Town and the accumulation of pollutants over Cape Town. Chapter five presents the conclusion of the study and offers some recommendations for future studies.

Chapter Two: Literature review

2.0 Introduction

This chapter reviews previous studies on pollutants in Cape Town and South Africa in general. The review focuses on the history of air pollution problems in Cape Town, the role of atmospheric conditions on air pollution in Cape Town, and modelling of pollutant transports in South Africa, and a review of the development of the regional climate model used in the study.

2.1 The history and sources of air pollution in Cape Town

The problem of air pollution in Cape Town is not new. Previous studies show that this issue can be dated back to the late 1960s, when the thick black smog from power stations and coal-burning locomotives were the major problem (Jury et al. 1990:7; Mauderly & Samet 2009:5; Smith & Mueller 2010:4932). In 1968, both the closure of the power stations and the replacement of the coal-burning locomotives seemed to solve the problem of the thick black smog; but then, the brown haze pollution problems emerged (Wicking-Baird et al. 1997:98). The brown haze is predominantly observed in winter (mainly from April to September) over Cape Town. Its formation is attributed to strong temperature inversions and windless conditions that prevail during these months. When this occurs, it is associated with bad odour and poor visibility, especially in the centre of Cape Town, where the levels of human activities are higher than those in the rural areas (CCT 2005:16). Kalognomou (2009:75) showed that brown haze can be related to emissions of pollutants from the following human activities in the city:

- **Motor vehicle emissions:** PM emitted from diesel vehicles; lead (Pb) from wear and tear of tyres; and carbon and hydrocarbons from incomplete combustion of fuel (Kalognomou 2009:75).
- **Industrial emissions:** lead, hydrocarbon and other heavy metals from refineries, chemical producing companies, steel mills, smelters, cement manufacturing, paper manufacturing, brickworks, inter alia, and emissions resulting from the burning of industrial wastes (Kalognomou 2009:75).

- **Domestic activities in residential areas:** suspended particles, carbon monoxide, sulphur dioxide, inter alia, from both formal and informal settlements, but especially in the informal settlements due to cooking, heating and the burning of household waste (Kalognomou 2009:75).

- **Agricultural emissions:** from residual waste burning, bush burning and crop spraying. An example of such emissions is a highly reactive compound called isoprene. Its emission from certain types of vegetation is believed to play an important role in both urban and rural ozone formation (Trainer et al 1987; Chameides, et al 1988; Sillman et al 1990).

Wicking-Baird et al. (1997:38) showed that emissions from road transport are the single largest source of primary NO_x, PM10, PM2.5 and volatile organic compound (VOC) emissions comprising 65.7%, 52.6%, 42.5% and 69.2% of the total emissions respectively. They showed that oil refinery, heavy fuel oil boilers and the use of coal for industrial and commercial purposes are the largest contributors to the total SO_2 emissions in the city.

Walton (2005:90) identified the Caltex Oil Refinery and the Consol Glass as the two major point sources of pollution in the city, while Cape Town International Airport, Cape Town Central Business District, the townships of Khayelitsha and Mitchell's Plain are the major point sources in the area. However, these previous studies did not investigate the contribution to the poor air quality in the city from emissions outside the city. Since wind often transports secondary pollutants, like HNO_3 (which causes health impairment), far from their original sources, it is important to examine the contribution of the transported pollutants to the air quality problem in Cape Town from remote sources in South Africa. The present study addresses the transport of NO_x and HNO_3 from sources outside CT, which might contribute to the pollution in CT.

2.2 The role of atmospheric conditions on air pollution in Cape Town

Many studies (i.e., Preston-Whyte, Diab & Tyson 1977; Jury et al. 1990) have indentified and described the meteorological factors that make CT vulnerable to air pollution. The location of CT (33.9^{o}S, 18.4^{o}E) at the south-western tip of Africa influences the wind pattern. The city is bordered by the Table Mountain complex to the south-west, False

Bay to the south, and Table Bay to the west; hence, calm conditions are sometimes produced over the city under stagnant anti-cyclonic flows. The subsidence temperature inversion suppresses vertical exchange of air and pollutants during most periods of the year. In addition, cooling at night produces a stable layer at the surface to form surface inversion, which prevents the vertical dispersion of pollutants during the early mornings. The South Atlantic anti-cyclone and the cold Benguela Current induce surface inversion, which strengthens over Cape Town (Preston-Whyte et al. 1977). Owing to the temperature contrast between the cold Benguela Current and the warm land, a weak sea-breeze develops during the day and traps pollutants within the Cape Town basin. Berg wind, which occurs when a high-pressure system over Kwazulu-Natal is associated with a high-pressure system over the Western Cape with an approaching cold front, favour brown haze episodes because, the warm north-easterly reduces dew point temperature during the night (Jury et al. 1990). Consequently, extreme high pollution events occur from April to September; and whenever the brown haze occurs during this period, it extends over most of CT and shifts according to the prevailing wind direction (Wicking-Baird et al., 1997:38).

2.3 Monitoring and Modelling of Air Pollution

Monitoring and modelling of air pollution are essential to discover and address pollution problems. Air pollution monitoring can be made directly using continuous measurement instrumentation or manual methods, or remotely using optical sensing systems (Walton 2005:4). Monitoring activities are typically separated into two classifications- source monitoring and ambient air monitoring. Source monitoring involves the measurement of emissions directly from a fixed or mobile emission source, typically in a contained duct, vent, stack or chimney. Stationary source data is used to determine control technology performance, confirm if the established permit limits are being met, and also used as input for the ozone and/or health risk prediction models. Major stationary sources may have continuous emissions monitors (CEMs) installed, to report real-time emissions, based on pre-established reporting cycles. Ambient air monitoring involves the measurement of specific pollutants present in an immediate surrounding atmosphere. Most urban areas often operate several ambient air monitoring instruments, each dedicated to measuring specific target pollutants.

In Cape Town, monitoring of air quality started in the late 1950s, with the introduction of the first monitoring station measuring SO_2 and smoke (Wicking Baird *et al.* 1997, 37-38).

The city has implemented an ambient air quality monitoring network, consisting of thirteen continuous monitoring stations and thirty eight analysers operating across the 500 km^2 metropolitan areas, to continuously assess real-time concentrations of critical pollutants such as carbon monoxide, carbon dioxide, sulphur dioxide and oxides of nitrogen in the atmosphere (Linde & Ravenscroft 2003). The city monitors the concentration levels of the following pollutants: lead (Pb), oxides of nitrogen (NO_x), ozone (O_3), particulate matter (PM), and sulphur dioxide (SO_2), with volatile organic compounds being monitored in specific surveys (CCT 2001). Wicking-Baird et al. (1997:vi) suggested that air quality monitoring be expanded into informal areas and townships, and that a long term consideration should be given to improve diesel, petrol fuel oil formulation, in order to reduce emissions. An integrated air quality management system should be developed, as suggested in (Linde & Ravenscroft 2003; CCT 2001). Although data from the monitoring station are utilised in this study, they are not sufficient for the study.

As an alternative to (or in conjunction with) direct monitoring, atmospheric-chemistry models are often used to simulate the emission, dispersion, transport, chemistry and deposition of the atmospheric pollutants. Atmospheric-chemistry models simulate these processes, by solving sets of numerical equations over complex terrain. The atmosphere module usually solves a complete set of hydrodynamic and thermodynamic equations to produce meteorological fields needed for dispersion and chemistry calculations. The dispersion calculations follow different approaches. One approach is to use the standard Gaussian dispersion model, as described by Hunt et al (1979:1227-1239), Misra (1980:397), Egan (1984:3-28), Andr´en (1987:1045-1058) and Enger (1990a:2431-2446). Significant deviations from idealized conditions introduce limitations on the validity of Gaussian models, because model uncertainties might become too large (Abiodun & Enger 2002:1589). These exceptional conditions are, for instance, near-calm, extremely stable, convective conditions, very irregular and rugged terrain. Hence, Gaussian models are not suitable for Cape Town. Another approach is to use Lagrangian particle-dispersion models. Atmospheric dispersion in a Lagrangian model is simulated by tracing a large set of particles driven by wind and turbulence fields predicted by the atmospheric model. Subsequent positions of each particle representing a discrete element of pollutant mass are computed from the relations. Examples of such models are described in Lamb (1979) and Uliasz (1994). A third approach is to use an Eulerian diffusion model, which involves starting from the mass with continuity equation. A first-order closure model for

complex terrain was used by Segal et al (1982:1381-1397) to study dispersion in the Greater Chesapeake Bay area. Enger (1986:879-894) has shown the capability of a second-order closure dispersion model in simulating observed dispersion features in a CBL. The model was also used to simulate dispersion in complex terrain in Enger (1990b:2447-2455), Enger and Koraˇcin (1995:2449-2465), and Abiodun and Enger (2002:1589). However, observation data from air quality monitoring network are usually used to establish the credibility of the air quality simulation by the atmospheric-chemistry models. This approach is adopted in this study.

2.4 Modelling the Transport of air pollutants in South Africa

Many studies have applied atmospheric models to study transports of pollutants in South Africa, and the targets of such studies have been on the transport of pollutants from the Mpumalanga Highveld - the most polluted area in South Africa. The Mpumalanga Highveld accounts for 90% of South Africa's emission of nitrogen oxides and other gases (Collett, Piketh & Ross 2010). Air pollution issues in South Africa were only brought to the public attention in the late 1980s, because of the concerns expressed over the high emissions from industries in the Highveld region. Van Tienhoven (1999) showed that South Africa is among the top ten countries contributing to the global greenhouse effect, and accounts for the 15% of the greenhouse gas emissions for the African continent. Most of South Africa's coal is burned on the Highveld in industrial plants such as petrochemical work stations, smelters, manufacturing plants and power plants (van Tienhoven, 1999). Van der Merwe (1998:5) employed a trajectory model to investigate the dispersion of SO_2 over the Highveld up to 600 km from the source, to assess the distribution of SO_2 and SO_4 under the major circulation patterns and found that the area affected was greater than previously thought. Piketh et al. (2002), and Freiman and Piketh (2003) used the trajectory models' low resolution re-analysis data to study the regional transport and recirculation of pollutants emitted from the Highveld. As such, they showed that most of the pollutants from the Highveld pollution are transported to the Indian Ocean by the westerlies at 700 hPa.

However, since the Mpumalanga Highveld is located north-east of Cape Town, a persistent low-level north-easterly flow over South Africa can transport the pollutants from the Highveld to Cape Town. Such a transport may not be captured by the previous

studies, which used low resolution atmospheric data in trajectory models. Freiman and Piketh (2003) criticised trajectory models, because, the models are of limited use under turbulent conditions. More so, the trajectory models cannot account for chemical reactions that occur among the pollutants during the transports, making it difficult to account separately for the concentration of primary and secondary pollutants. Meanwhile, in some cases, the concentration of the secondary pollutants may be higher than that of their precursors. In the present study, a high resolution atmospheric-chemistry Eulerian model that accounts for the influence of topography, atmospheric condition and chemical reactions among the atmospheric gases, is used to investigate the transported pollutants from the Mpumalanga Highveld to Cape Town.

Eulerian pollution models overcome the shortcomings of trajectory models (Jenner 2013). Zunckel et all (2004b) used an Eularian model to investigate pollutant deposition and showed that the results agreed with observations. The authors further used the model to show that the concentrations of atmospheric pollutants in any location in southern Africa may be linked to emissions from other parts of the region. Some studies also applied Eulerian models to study pollution over CT. The Cape Town Air Quality Monitoring Group employed an atmospheric-chemistry-transport model, in addition to ambient monitoring, to study the problem of continually high levels of PM10 (particulate matter with a diameter less than 10 microns) (Muchapondwa 2010). Zunckel et al. (2004b) developed a photochemical dispersion model, the Dynamic Air Pollution Prediction System (DAPPS), to predict the ambient pollution based on local emissions sources and meteorological forecasting, but the project was abandoned due to a lack of funding.

Walton (2005:30) used an Eularian model to study the contribution of major local sources to Brown Haze and to investigate the meteorological conditions that contributed to Brown Haze formation. However, the focus of Walton (2005:30) was on the influence of local emissions on Cape Town's pollution. Eularian models can be run at a regional scale to incorporate synoptic conditions and they provide an ideal tool to investigate the source of pollutants that may be remote as well as local in origin. This present study adopts an Eulerian model (called RegCM) to study the local origins of the pollutants in CT and the transport of pollutants from the Mpumalanga Highveld.

2.5 Modelling atmospheric-chemistry with Regional Climate Model (RegCM)

Various studies have used RegCM, a dynamic regional climate model developed and maintained by the International Centre for Theoretical Physics (ICTP), for high resolution regional climate studies over different region of interest (Sylla et al & Bi 2009:231; Giorgi & Anyah 2012a:3). The first version of RegCM was built upon the NCAR-Pennsylvania State University (PSU) Mesoscale Model version 4 (MM4) in the late 1980s (Dickinson et al 1989:383; Giorgi, 1990:941). Since then RegCM has undergone series of improvement. The latest version of the model is version 4, which is used in this study. RegCM allows online coupling of atmospheric and chemistry parameters. Like any complex atmospheric model, the latest version of RegCM comprises of dynamic and physics components. While the dynamic component of the latest version of RegCM has not changed much from that of the first version, the physics component has changed considerably. The dynamic and physics components of the latest version is reviewed here.

2.5.1 The dynamic equations of RegCM

The dynamic equations and numerical discretisation in RegCM are described by Grell, Dudhia and Stauffer (1994:121). The dynamic equations include the horizontal momentum equations, continuity equation, thermodynamic equation (Elguindi, Bi, Giorgi, Nagarajan, Pal, Solmon, Rauscher & Zakey 2010:10-11). Elguindi et al. (2010:8) shows that the vertical coordinate of RegCM is terrain-following, meaning that the lower grid levels follow the terrain, while the upper surface is flatter and the intermediate levels progressively flatten, as the pressure decreases toward the top of the model. The horizontal grid has an Arakawa-Lamb B-staggering of the velocity variables with respect to the scalar variables. The scalars are defined at the center of the grid box, while the eastward and northward velocity components are co-located at the corners. However, the finite differencing in the model is crucially dependent upon the grid staggering, whereas gradients or averaging are the available terms in the equation. RegCM has a choice of four map projections- Lambert Conformal, for mid-latitudes, Polar Stereographic, for high latitudes, Normal Mercator, for low latitudes, and Rotated Mercator, for extra choice. The projections in the model preserve the shape of small areas, but the grid length varies across the domain to allow a representation of a

spherical surface on a plane surface. Map-scale factors need to be accounted for in the model equations, wherever horizontal gradients are used.

2.5.2 The physics component of RegCM

RegCM uses parameterisation schemes to represent different atmospheric processes in the atmosphere. These include radiation, land surface, planetary boundary layer, convective precipitation, large scale precipitation, ocean flux, sea surface temperature, and atmospheric chemistry. The model has alternative parameterisation schemes for some processes, but only one option for others.

2.5.2.1 Radiation

RegCM has one option for radiation. It uses the radiation scheme of the NCAR CCM3, which is described in Kiehl, Hack, Bonan, Boville, Brigleb, Williamson and Rasch (1996:1-139). In the scheme, the solar component, which accounts for the effect of O_3, H_2O, CO_2, and O_2, follows the d-Eddington approximation of Kiehl et al. (1996: 52-57). It includes 18 spectral intervals from 0.2 to 5 μm. The cloud scattering and absorption parameterization follow that of Slingo et al (1989), whereby the optical properties of the cloud droplets (extinction optical depth, single scattering albedo, and asymmetry parameter) are expressed in terms of the cloud liquid water content and an effective droplet radius. When cumulus clouds are formed, the gridpoint fractional cloud cover is such that the total cover for the column extending from the model-computed cloud-base level to the cloud-top level (calculated assuming random overlap) is a function of the horizontal gridpoint spacing. The thickness of the cloud layer is assumed to be equal to that of the model layer, and different cloud water content is specified for middle and low clouds.

2.5.2.2 Land surface model

RegCM has two model (parameterization) options called Biosphere-Atmosphere Transfer Scheme (BATS) and Common Land Model (CLM) for land surface process. BATS is a surface package designed to describe the role of vegetation and interactive soil moisture in modifying the surface-atmosphere exchanges of momentum, energy, and water vapor (Dickinson et al & Wilson 1986:1). The model has a vegetation layer, a snow layer, a surface soil layer, 10 cm thick, or root zone layer, 1-2 m thick, and a third deep soil layer,

3 m thick. Prognostic equations are solved for the soil layer temperatures using a generalisation of the force-restore method of Deardoff (1978:1890). The temperature of the canopy and canopy foliage is calculated diagnostically, via an energy balance formulation including sensible, radiative, and latent heat fluxes. The soil hydrology calculations include predictive equations for the water content of the soil layers. These equations account for precipitation, snowmelt, canopy foliage drip, evapo-transpiration, surface runoff, infiltration below the root zone, and diffusive exchange of water between soil layers. The soil water movement formulation is obtained from a fit, to result from a high-resolution soil model- Dickinson (1984), and the surface runoff rates are expressed as functions of the precipitation rates and the degree of soil water saturation. Snow depth is prognostically calculated from snowfall, snowmelt, and sublimation. Precipitation is assumed to fall in the form of snow, if the temperature of the lowest model level is below 271 K. Sensible heat, water vapor, and momentum fluxes at the surface are calculated using a standard surface drag coefficient formulation based on surface-layer similarity theory. The drag coefficient depends on the surface roughness length and the atmospheric stability in the surface layer. The surface evapotranspiration rates depend on the availability of soil water. Biosphere-Atmosphere Transfer Scheme (BATS) has 20 vegetation types (soil textures ranging from coarse (sand), to intermediate (loam), fine (clay) and different soil colours (light to dark) for the soil albedo calculations). These are described in Dickinson et al. (1986:1-62).

CLM is the land surface model developed by the National Centre of Atmospheric Research (NCAR) as part of the Community Climate System Model (CCSM). This is described in detail in Collins, Bitz, Blackmon, Bonan, Bretherton, Carton, Chang, Doney, Hack, Henderson, Kiehl, Large, Mckenna, Santer and Smith (2006:2122-2142). CLM contains five possible snow layers, with an additional representation of trace snow and ten unevenly spaced soil layers with explicit solutions of temperature, liquid water and ice water in each layer. To account for land surface complexity within a climate model grid cell, CLM uses a tile or mosaic approach to capture surface heterogeneity. Each CLM grid cell contains up to four different land cover types (glacier, wetland, lake, and vegetated), where the vegetated fraction can be further divided into 17 different plant functional types. Hydrological and energy balance equations are solved for each land cover type and aggregated back to the gridcell level. CLM requires several time-invariant surface input parameters- Soil color, Soil texture, Percent cover of each land surface

type, Leaf and stem area indices, Maximum saturation fraction, and Land fraction (Lawrence & Chase 2007:1-27). Table 3 shows the resolution for each input parameter used at the regional scale in RegCM-CLM, compared to resolutions typically used for global simulations. The resolution of surface input parameters was increased for several parameters to capture surface heterogeneity, when interpolating to the regional climate grid. Similar to Lawrence and Chase (2007:1-27), the number of soil colours was extended from 8 to 20 classes, to resolve regional variations. The second modification was to update the soil moisture initialization based on a climatological soil moisture average (Giorgi & Bates 1989:2325–2347) over the use of constant soil moisture content throughout the grid generally used for global CLM. By using a climatological average for soil moisture, model spin-up time is reduced, with regards to deeper soil layers. The third modification to the CLM is the inclusion of a mosaic approach for grid cells that contain both land and ocean surface types. With this approach, a weighted average of necessary surface variables was calculated for land/ocean grid cells, using the land fraction input dataset. This method provides a better representation of coastlines, using the high-resolution land fraction data (Olesonet al 2004).

2.5.2.3 Land surface model

RegCM uses the planetary boundary layer scheme developed by Holtslag et al (1990:1561-1575). The scheme is based on a non-local diffusion concept that takes into account, the counter gradient fluxes resulting from large-scale eddies in an unstable, well-mixed atmosphere. Holtslag et al. (1990:1561-1575), and Holtslag and Boville (1993:1825-1842) provide detailed description and equation of the scheme.

2.5.2.4 Convective precipitation scheme

RegCM4 has three convective precipitation schemes, namely: Modified-Kuo scheme Anthes (1977), Grell scheme Grell (1993) and MIT-Emanuel scheme (Emanuel 1991; Emanuel and Zivkovic-Rothman 1999). Convective activity in the Kuo scheme is initiated when the moisture convergence in a column exceeds a given threshold and the vertical sounding is convectively unstable. A fraction of the moisture convergence moistens the column and the rest is converted into rainfall. The latent heating resulting from condensation is distributed between the cloud top and bottom by a function that allocates the maximum heating to the upper portion of the cloud layer. To eliminate numerical point

storms, a horizontal diffusion term and a time release constant are included, so that the redistributions of moisture and the latent heat release are not performed instantaneously (Giorgi & Bates 1989; Giorgi & Marinucci 1991). The Grell scheme (Grell 1993), considers clouds as two steady-state circulations- an updraft and a downdraft. No direct mixing occurs between the cloudy air and the environmental air, except at the top and bottom of the circulations. The mass flux is constant with height and no entrainment or detrainment occurs along the cloud edges. The originating levels of the updraft and downdraft are given by the levels of maximum and minimum moist static energy, respectively. The Grell scheme is activated when a lifted parcel attains moist convection. Condensation in the updraft is calculated by lifting a saturated parcel. The downdraft mass flux depends on the updraft mass flux. The MIT-Emanuel scheme is the Massachusetts Institute of Technology (MIT) scheme (Emanuel, 1991: 2313-2335; Emanuel and Zivkovic-Rothman 1999:1766-1782). The scheme assumes that the mixing in clouds is highly episodic and inhomogeneous (as opposed to a continuous entraining plume) and considers convective fluxes based on an idealized model of sub-cloud-scale updrafts and downdrafts. Convection is triggered when the level of neutral buoyancy is greater than the cloud base level. Between these two levels, air is lifted and a fraction of the condensed moisture forms precipitation, while the remaining fraction forms the cloud. The cloud is assumed to mix with the air from the environment, according to a uniform spectrum of mixtures that ascend or descend to their respective levels of neutral buoyancy. The mixing entrainment and detrainment rates are functions of the vertical gradients of buoyancy in clouds. The fraction of the total cloud base mass flux that mixes with its environment at each level is proportional to the undiluted buoyancy rate of change with altitude. The cloud base upward mass flux is relaxed towards the sub-cloud layer quasi equilibrium.

2.5.2.5 Large-Scale Precipitation Scheme

Sub-grid Explicit Moisture Scheme (SUBEX) is used to handle non-convective clouds and precipitation resolved by the model. This is one of the new components of the model. SUBEX accounts for the sub-grid variability in clouds by linking the average grid cell relative humidity to the cloud fraction and cloud water, following the work of Sundqvist, Berge and Kristjansson (1989:2698-2712).

2.5.2.5 Aerosols and Chemistry

RegCM has undergone series of development in the representation of aerosol and chemistry modules (Giorgi, Coppola, Solmon, Mariotti, Sylla, Bi, Elguindi, Diro, Nair, Giuliani, Turuncoglu, Cozzini, Güttler, O'Brien, Tawfik, Shalaby, Zakey, Steiner, Stordal, Sloan, Bran 2012b:7-29). Solmon, Giorgi and Liousse (2006:51-72) first implemented a first-generation aerosol model including SO_2, sulfates, organic carbon, and black carbon. Zakey, Solmon and Giorgi (2006:4687–4704) then added a 4-bin desert dust module, while Zakey, Giorgi and Bi (2008) implemented a 2-bin sea salt scheme. The dust emission scheme accounts for sub grid emissions by different types of soil, and the soil texture distribution has been updated according to Laurent et al. (2008). The dust emission size distribution can now also be treated according to Kok (2011). When all aerosols are simulated, 12 additional prognostic equations are solved in RegCM4, including the transport by resolvable scale winds, turbulence and deep convection, sources, and wet and dry removal processes. The aerosols are radiatively interactive, both in the solar and infrared regions of the radiation spectrum. Various versions of this aerosol scheme were used to simulate the regional climatic effects of sulfate aerosols in China et al 2002), Saharan dust (Konare, Zakey, Solmon, Giorgi, Rauscher, Ibrah & Bi 2008; Solmon, Mallet, Elguindi, Giorgi, Zakey & Konaré 2008:1-6), Asian and Mediterranean dust (Zhang et al 2010), and African biomass burning aerosol (Tummon et al 2010; Malavelle et al 2011).

RegCM4 uses a set of gas-phase chemistry mechanisms of different complexity- the carbon-bond mechanism CBM-Z (Zaveri & Peters 1999), an extended version of the GEOS-Chem mechanism and the comprehensive RADM2, together with 2 numerical solvers- the Rosenbrock solver and a fast solver based on radical balance. These modules were tested by Shalaby et al. (unpubl.) in the simulation of the extreme ozone event of the summer 2003 over Europe. They showed that the combination of the CBM-Z, which treats 52 species for 132 reactions and requires the inclusion of 24 new prognostic tracers, along with the radical balance solver, provided the most computationally efficient simulation with a good representation of tropospheric chemistry. The chemistry solver is completed by a dry deposition scheme adapted from Zhang, Brook and Vet (2003) and an emission pre-processing interface capable of handling different emission inventories from the Global Emission Inventory Activity. When the CLM

land surface scheme is activated, biogenic emissions can be calculated online, using the MEGAN module (Guenther, Karl, Harley, Wiedinmyer, Palmer & Geron 2006).

Chapter Three: Methodology

3.0 Introduction

This thesis used meteorological and pollution data from four stations within the Cape Town Air Quality Monitoring Network (Fig. 3.2). The network consists of 12 stations within 500 km^2 area and measures ambient concentrations of selected pollutants considered hazardous to human health and ecology (CCT 2005), as well as relevant meteorological parameters that might elucidate high concentrations.

3.1 Observed data

The stations with relevant observations for the period of study are City Hall, Goodwood, Bothasig, and Tableview (see Fig. 3.1 and Fig. 3.2 below). Vehicular emissions are the prime source for the City Hall station, which is located opposite the city's busy taxi rank, bus station and rail terminus. Goodwood is a mixed residential and commercial area with nearby industries to the south-east and south-west. The nearby national road, the N2, carries commuter traffic from Cape Town's northern suburbs to the City, and another busy national road, the N7, passes along the south side of this area. The road traffic near these two stations is congested during the morning and evening commute. Although situated near arterial roads, traffic contributes next to nothing to the source of data for the Bothasig and Tableview monitors located near the coast and in close proximity to each other.

The data analysed for this study included the average hourly interval concentrations of NO, NO_2 and NO_x, wind speed, wind direction and temperature over ten years (2000 – 2009). The data were analysed to identify temporal variation of concentrations and associated atmospheric conditions. Diurnal variation was analysed to investigate the concentration peaks and the contribution of the atmospheric conditions. Monthly mean concentrations of pollutants and climatological variables were used to identify the influence of seasonal variations. Monthly temperature and rainfall data from the Climate Research Unit (CRU 2012; Mitchell & Jones 2005) were analysed to supplement the station data in validating the model simulation.

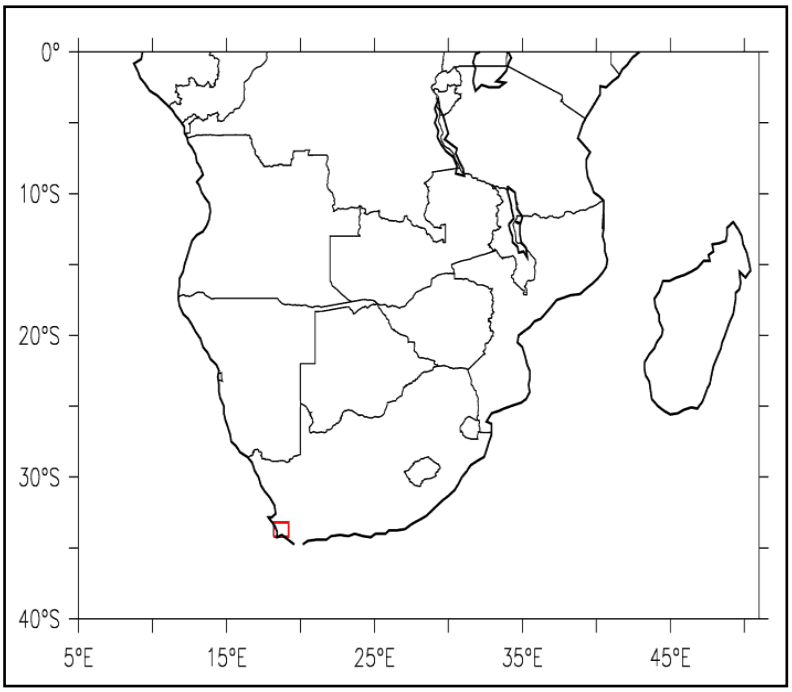

Figure 3. 1: Map of southern Africa showing the Cape Town area (red box) at the south-western tip of South Africa.

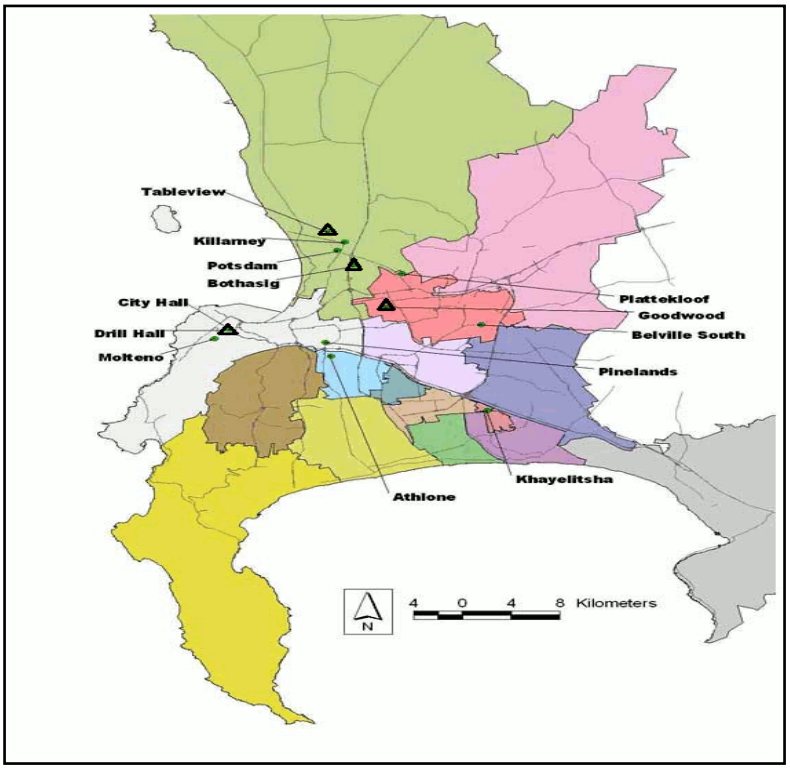

Figure 3.2: The Cape Town Air Quality Network showing the location of observation stations. The locations of the four stations (Bothasig, City Hall, Goodwood and Tableview) used in the study are indicated with triangles (Δ) Source: **www.capetown.co.za.**

3.2 Model description and simulation set-up

The International Centre for Theoretical Physics (ICTP) Regional Climate Model (version 4) with chemistry (hereafter, RegCM) was used to simulate the climate and pollution transport over southern Africa (Fig. 3.3). The model allows online coupling of atmospheric and chemistry parameters. The climate component has been tested over southern Africa (Sylla et al. 2009:231-247). RegCM is a hydrostatic, sigma-coordinate following model (Pal, Giorgi, Bi, Elguindi, Solmon, Gao, Rauscher, Francisco, Zakey, Winter, Ashfaq, Syed Bell, Diffenbaugh, Karmacharya, Konaré, Martinez, da Rocha, Sloan & Steiner 2007:232; Giorgi & Anyah 2012a:3-6). The model has various options for physics and chemistry parameterisations. For the present study, the model used the community climate model CCM3 (Kiehl, et al. 1996:55-132) radiation scheme for radiation calculations, the mass-flux cumulus scheme (Grell et al., 2005) with Fritsch and Chappell (1980) closure for convection, and the Holtslag and Boville (1993:1825-1842) scheme for planetary boundary layer parameterisation. Surface layer land-atmosphere interactions were represented with BATS1E (Biosphere-Atmosphere Transfer Scheme) (Dickinson, Henderson-Sellers & Kennedy 1993), which is based on Monin Obukhov similarity relations (Monin & Obukhov 1954). For the chemistry routines, the photochemical Carbon Bond Mechanism-Z (CBM-Z) (Zaveri & Peters, 1999) was used. Photolysis is based on the Tropospheric Ultraviolet-Visible Model (TUV) scheme developed by Madronich and Flocke (1999). For dry deposition, the model used the CLM4 (Community Land Model 4) developed after Wesley (1989), and wet deposition follows the MOZART global model (Emmons, Walters, Hess, Lamarque, Pfister, Fillmore, Granier, Guenther, Kinnison, Laepple, Orlando, Tie, Tyndall, Wiedinmyer, Baughcum & Kloster 2010:43-67). Shalaby, Zakey, Tawfik, Solmon, Giorgi, Stordal, Sillman, Zaveri, and Steiner (2012:149-187) presents a detailed description of the gas-phase chemistry in RegCM.

The RegCM simulation was set up with a 35 km horizontal resolution. The simulation domain centres on 33°S and 24°E and extends with the Lambert conformal projection from 16.62°W to 54.41°E and from 10.5°S to 40.45°S (Fig. 3.3). In the vertical, the domain spans 18 sigma levels, with the highest resolution near the surface and the lowest resolution near the model top. Initial and lateral boundary meteorological conditions were provided by ERA-Interim 1.5° x 1.5° gridded re-analysis data from ECMWF (European Centre for Medium-Range Weather Forecasts). Emissions data with

a 1° x 1° resolution was provided by the RCP (Representative Concentration Pathways) global dataset, provided with standard RegCM package. The simulation covers a period of four years, three months (i.e., October 2000 - December 2004). The first three months' simulations were discarded as model spin-up, while the remaining four years' simulations were analysed for the study.

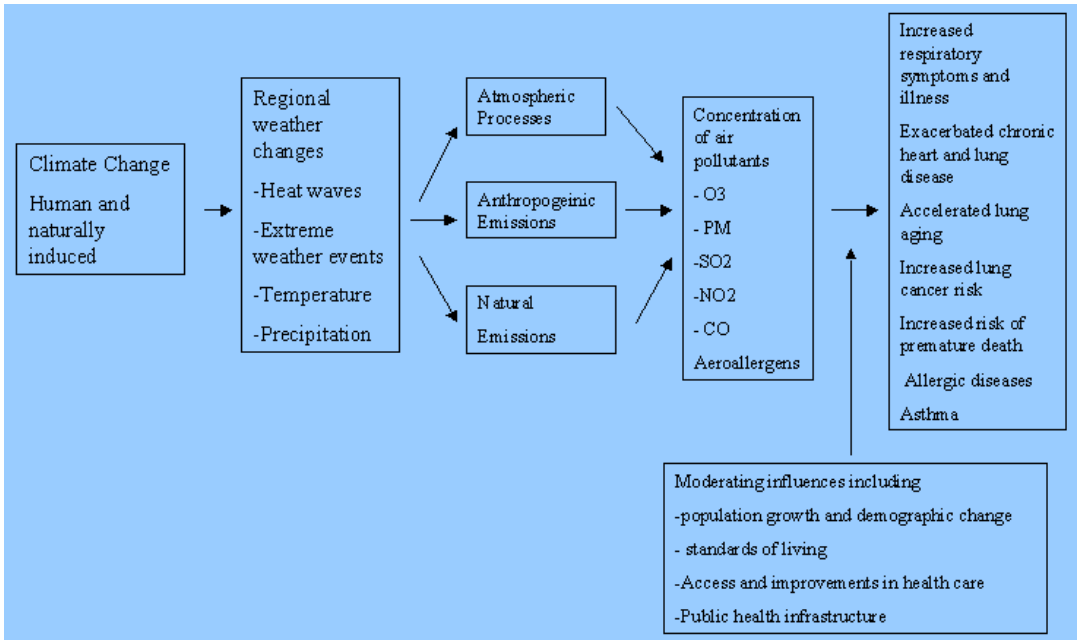

Figure 3.3: diagram of RegCM model incorporating both atmospheric and chemistry parameters inputs. Source (internet)

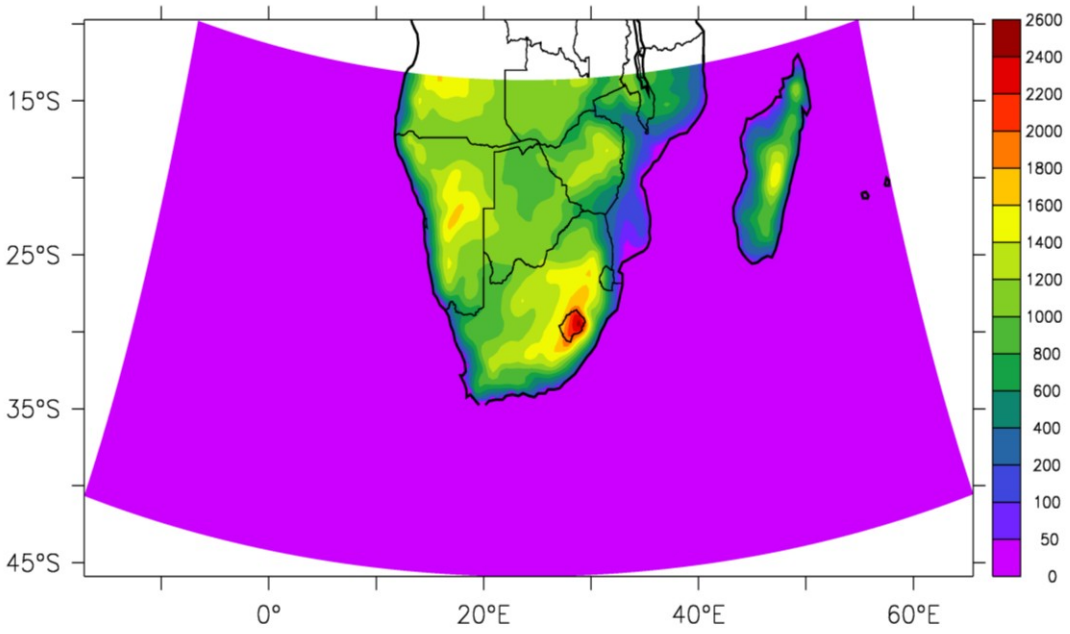

Figure 3.4: RegCM simulation domain indicating the topography of southern Africa as seen by the model (as simulated by me)

3.3 Pollutants flux budget

Flux budget analysis was use to calculate the net flux and to examine whether Cape Town is a source or sink for NO_x and HNO_3 during the extreme pollution events. The net flux (F_{Net}) over is defined as:

$$\mathbf{F_{Net} = (F_E - F_W) + (F_N – F_S);} \qquad \mathbf{(3.1)}$$

where F_E, F_W, F_N, and F_S are the pollutant fluxes at the east, west, north and south boundaries of Cape Town (Fig. 3.1), respectively. A positive zonal flux (F_E or F_W) implies a westerly pollutant flux (i.e., pollutant flux from a westerly direction), while a negative zonal flux means the opposite. A positive meridional flux (F_N or F_S) denotes a southerly pollutant flux (i.e., pollutant flux from the southern direction), while a negative zonal flux means the opposite. A positive net flux indicates a divergence of pollutants over the city, meaning that the city is a net source for pollutants. A negative net flux indicates a convergence (or an accumulation) of pollutants over the city, meaning that the city is a net sink for pollutants.

Chapter Four: Results and discussion

4.0 Introduction

This chapter presents and discusses the results of the thesis in three sections. The first section describes the temporal (diurnal and seasonal) variation of the observed pollutant concentration and meteorological variables at the four stations (City Hall, Goodwood, Bathasig and Tableview) within the city (see Fig. 3.2). The second section compares RegCM simulation (pollutant concentration and meteorological variables) with the observed data. The third section discusses the characteristics of the simulated NO_x (NO and NO_2) and HNO_3 over Cape Town.

4.1 Observed nitrogen oxides and atmospheric conditions

The diurnal variation and the seasonal variation of both the pollutant concentration and the meteorological variables observed at the City Hall, Goodwood, Bathasig and Tableview are presented and analysed in this section. These are needed to validate the modelling results presented in the following section.

4.1.1 Diurnal variation

The diurnal cycle of the NO, NO_2, NOx (Fig. 4.1) shows that the pollutants have the highest concentration at City Hall and the lowest concentration at Tableview. This is because City Hall is located in the heart of the city where emission of NO from daily anthropogenic activity (traffic, industrial, business) is greatest. The diurnal variation of NO concentration (Fig. 4.1a) shows two peaks (morning and evening) at City Hall but only one peak (morning) at other stations (Bothasig, Goodwood, and Tableview). The morning peaks (City Hall: 280 µg/m3; Goodwood: 120 µg/m^3; Bothasig: 60µg/m^3; and Tableview: 20 µg/m^3) occur at 8h00 SLT (Fig. 4.1a), while the evening peak (City Hall: 60µg/m^3) occurs at 16h00 SLT (Fig. 4.1a). Although Bothasig, Goodwood and Tableview show no evening peak, the NO concentration is higher in the evening (18h00 – 20h00) than in the afternoon. The morning and evening peaks at City Hall can be attributed to the high commuter traffic in the city because people rush to work and school in the morning (around 8h00 SLT) and return home in the evening (16h00 SLT). However, the concentration peak is higher in the morning than in the evening because the traffic rush

is greater in the morning as schools and offices open at the same time (8h00 SLT) but close at different times in the afternoon.

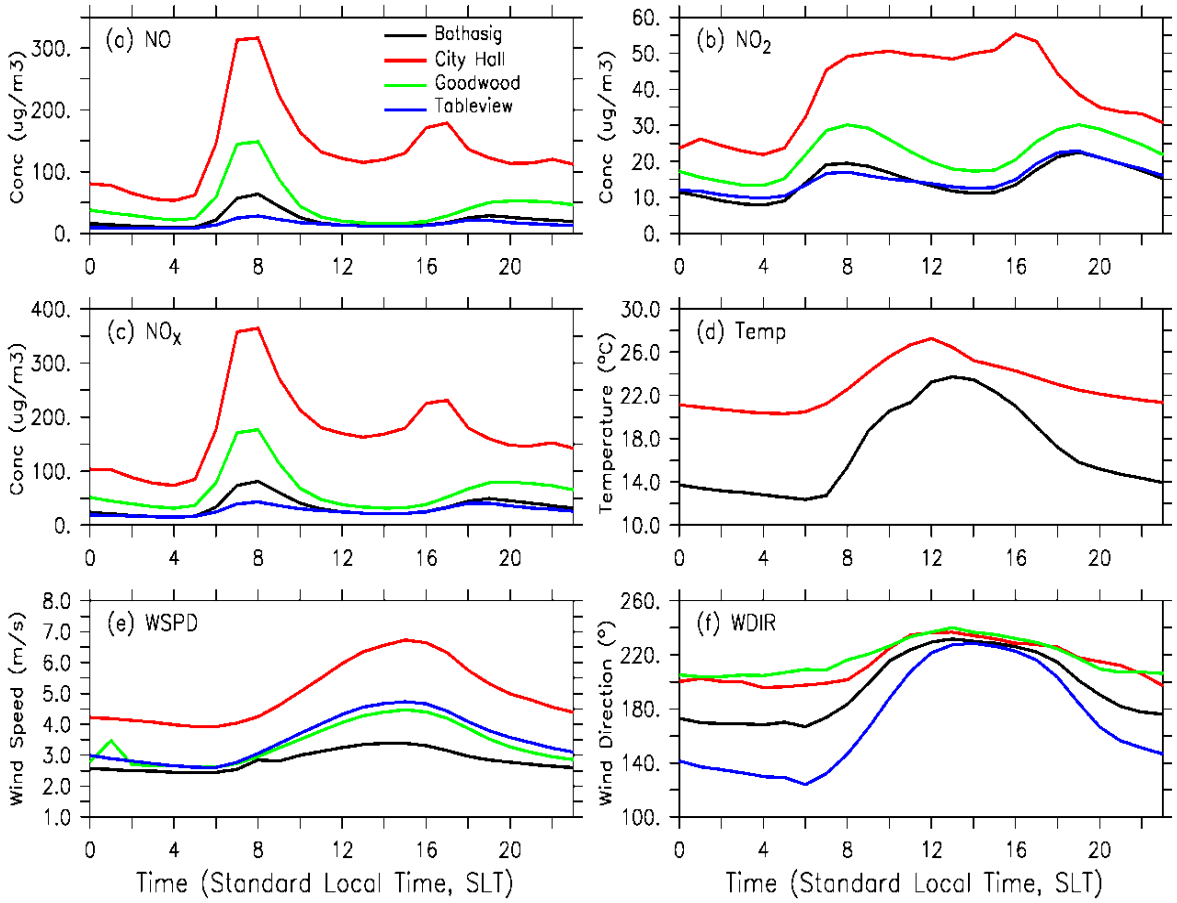

Figure 4. 1: Diurnal variation of observed (a) NO (b) NO_2 (c) NO_x (d) temperature (e) wind speed and (f) wind direction at four monitoring stations in Cape Town.

The diurnal variation of NO_2 (Fig. 4.1b) differs from that of NO. At City Hall, the diurnal variation of NO_2 shows no distinct peak; instead, it shows a uniform concentration (about 50 $\mu g/m^3$) during the day (08h00 – 18h00 SLT) (Fig. 4.1a), and a lower concentration (about 20 $\mu g/m^3$) at night. This could be explained as NO_2 is a secondary pollutant and not released directly. In contrast, the diurnal variation of NO shows two distinct peaks at other stations (Goodwood: 25 $\mu g/m^3$; Tableview and Bathasig: 18 $\mu g/m^3$), in the morning (8h00 SLT) and in the evening (19h00 SLT) (Fig.4.1a). However, at all stations, the NO_2 concentration is smaller than that of NO, possibly because NO_2 is a secondary reaction product of NO and oxygen (Eqn. 1.1); the reaction rate is slow and it depends on favourable atmospheric condition. Nevertheless, since the magnitude of NO concentration is about five times higher than that of NO_2, the diurnal variation of NOx ($NO + NO_2$) follows that of NO.

However, the diurnal variation of meteorological variables may also play an important role on the diurnal variation of the pollutants' concentration. The diurnal variation in wind speed (Fig. 4.1e) and surface temperature (Fig. 4.1d) may enhance the concentrations of the pollutants in the morning and lower it in the afternoon. For instance, the weak surface wind speed in the morning (Fig. 4.1e) may lead to accumulation and higher concentration of NO, while the higher wind speed in the afternoon may reduce NO concentration. Besides, in the morning, the surface inversion layer (induced by low surface temperature from the nocturnal radiation cooling) can inhibit vertical mixing of the NO. In the afternoon, the surface heating can increase the surface temperature; consequently the development of layers mixing will erode the inversion layer. Hence, pollutants trapped below the surface layer will rise and disperse, reducing the NO concentration in the afternoon. By contrast, the increase in NO_2 concentration in the afternoon may be attributed to an increase in temperature which can enhance the generation of more NO_2 due to chemical reaction (see Eqn. 1.1). This could further explain why NO_2 concentration is much higher at City Hall (where the maximum temperature is about 27^oC) than at Bothasig (where the maximum temperature is about 22^oC).

4.1.2 Seasonal variation

The concentration of the pollutants also varies with the seasons (Fig. 4.2). Since the anthropogenic emission of NO in CT hardly changes with the seasons, the seasonal variations of the atmospheric condition must play a major role in this variation of the

pollutants' concentration. At all stations, NO shows a maximum concentration (City Hall, 200 μg/m^3; Goodwood, 100 μg/m^3; Bothasig, 100 μg/m^3; Tableview, 30 μg/m^3) in early winter (June) and a minimum concentration (City Hall: 80 μg/m^3; Goodwood, Bothasig and Tableview: 20 μg/m^3) in summer (December – February). Nevertheless, the seasonal variation is most pronounced at Town Hall and least defined at Tableview (Fig. 4.1a). The occurrence of maximum concentration of NO in winter can be attributed to the weak wind speed and low surface temperature during this period, as both conditions do not favour the pollutant dispersion and its conversion to NO_2 through the reaction in equation (1.1).

The seasonal variation of NO_2 (and NO_x) is similar to that of NO, except that:

(i) the concentration of NO_2 is smaller than that of NO;
(ii) at Town Hall, the maximum concentration of NO_2 extends over more months (March – July) than that of NO; and
(iii) at Tableview, the maximum concentration of NO_2 is in March – May instead of in June (as for NO).

The occurrence of maximum concentration of NO_2 in March – July can be attributed to a balance between NO concentration and atmospheric condition that favours NO_2 production. For instance, less NO concentration limits the production of NO_2 in January (when the temperature is most favourable for the production), and less favourable atmospheric condition prevents the peak concentration of NO_2 in June, when the NO concentration reaches its peak.

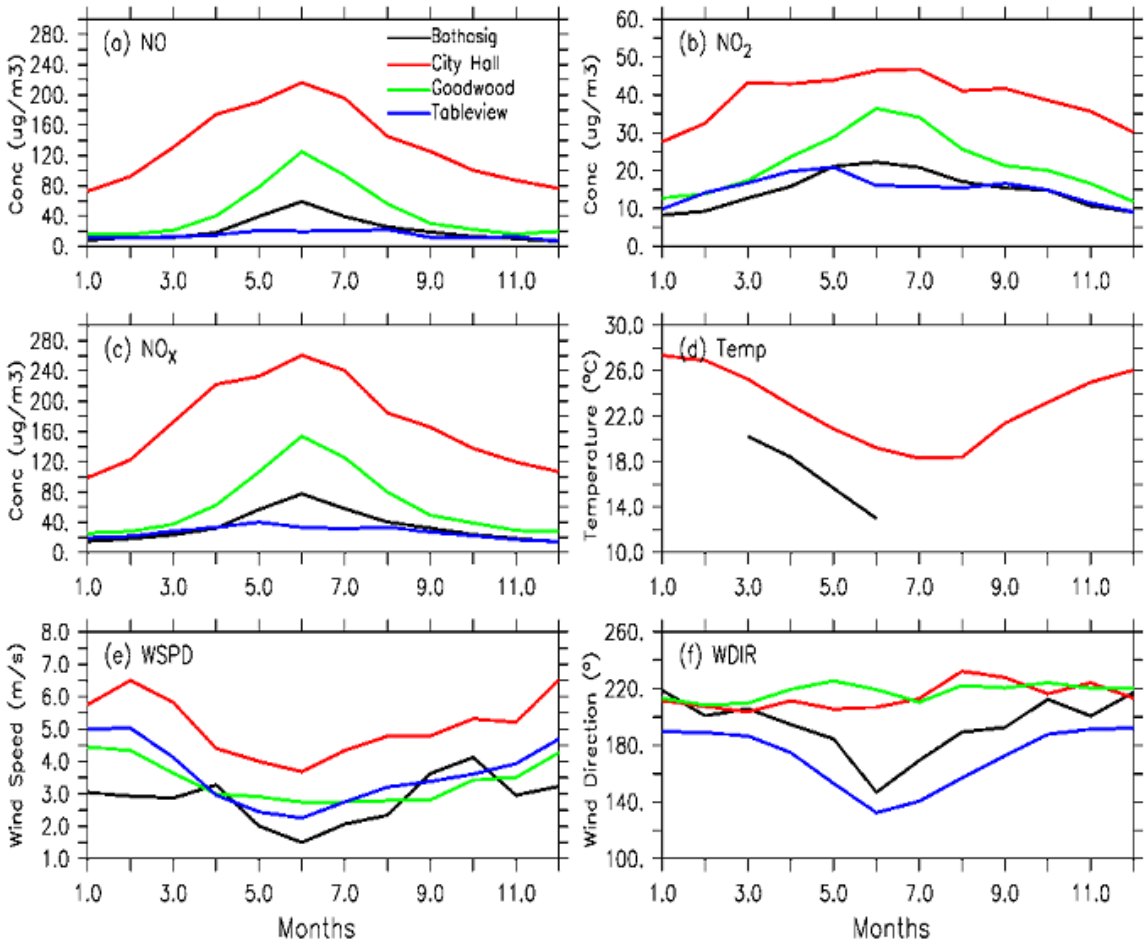

Figure 4.2: The seasonal variation of observed (a) NO (b) NO_2 (c) NO_x, (d) temperature (e) wind speed and (d) wind direction at four monitoring stations in Cape Town.

4.2 Model validation

The daily mean concentration of the simulated NO shows a weak correlation with the observed values and the standard deviation is lower than the observed (Fig. 4.3). The correlation coefficient is about 0.4 and the normalised standard deviation is 0.4. The simulated correlation between the observed and simulated NO_2 is also 0.4, but the normalised standard deviation (about 1.0) is much better than that of NO. The normalised standard deviation of NO_x (0.50) falls between those of NO and NO_2, but the correlation coefficient is also 0.4. There is a better correlation between the simulated and observed atmospheric variables than with the pollutants, suggesting that the weak correlation between the observed and simulated pollutant concentration may be due to the RegCM chemistry. However, the RegCM shows the best performance in simulating temperature; the correlation coefficient is 0.85 and the normalised standard deviation is 0.8.

The seasonal variation of the simulated pollutants concentrations resembles that of the observation, but with some biases in the values (Fig. 4.4). The model underestimates the concentrations of NO and NO_x in winter (May – August) and overestimates them in the other months. It underestimates NO_2 concentration in March – September and overestimates it in the other months. For all the pollutants, the highest bias in the simulation occurs in June and the lowest bias is in April or September. The peaks of the simulated concentrations (in April) are two months earlier than the observed (June). The decrease in the simulated pollutant concentration in winter may be attributed to the winter rainfall, which cleanses the atmosphere of any accumulated pollutant. The simulated rainfall and temperature show a good agreement with CRU observation, except that the model underestimates temperature in summer months, overestimates rainfall in winter and underestimates rainfall in winter. Another discrepancy between the simulation and observation is that the relationship between NO and NO_2 is stronger in the simulation than in observation.

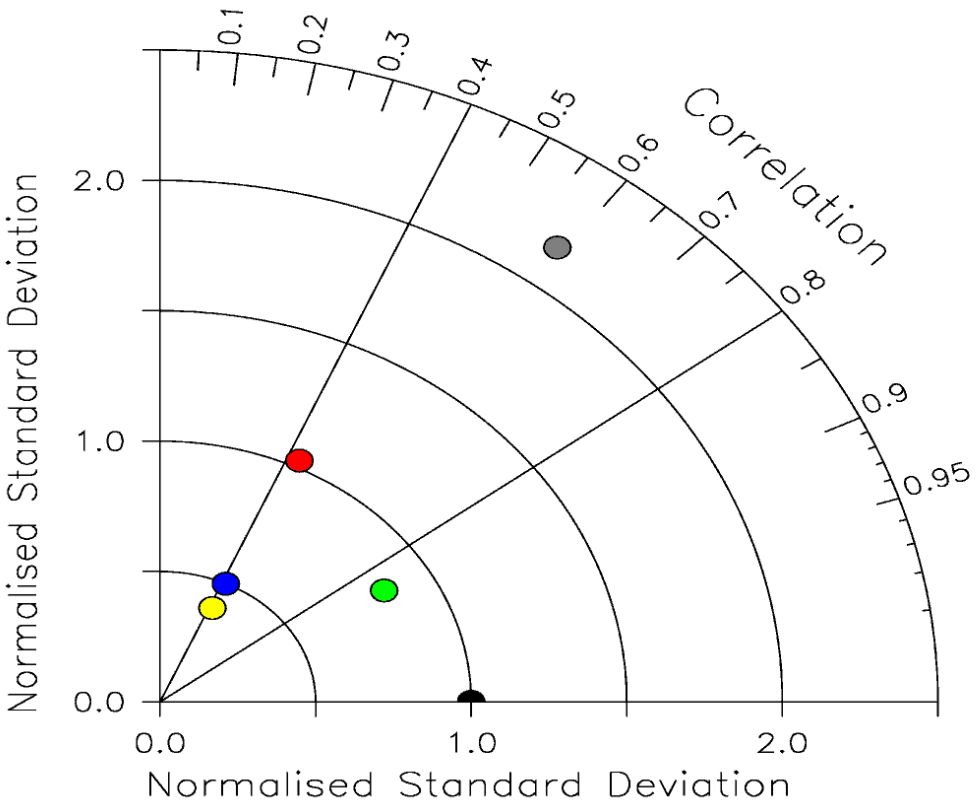

Figure 4.3: Comparison of the simulated (RegCM4) and observed daily mean concentration of NO (yellow), NO_2 (red) and NO_x (blue) temperature (green), and wind speed (grey). The observations are in black

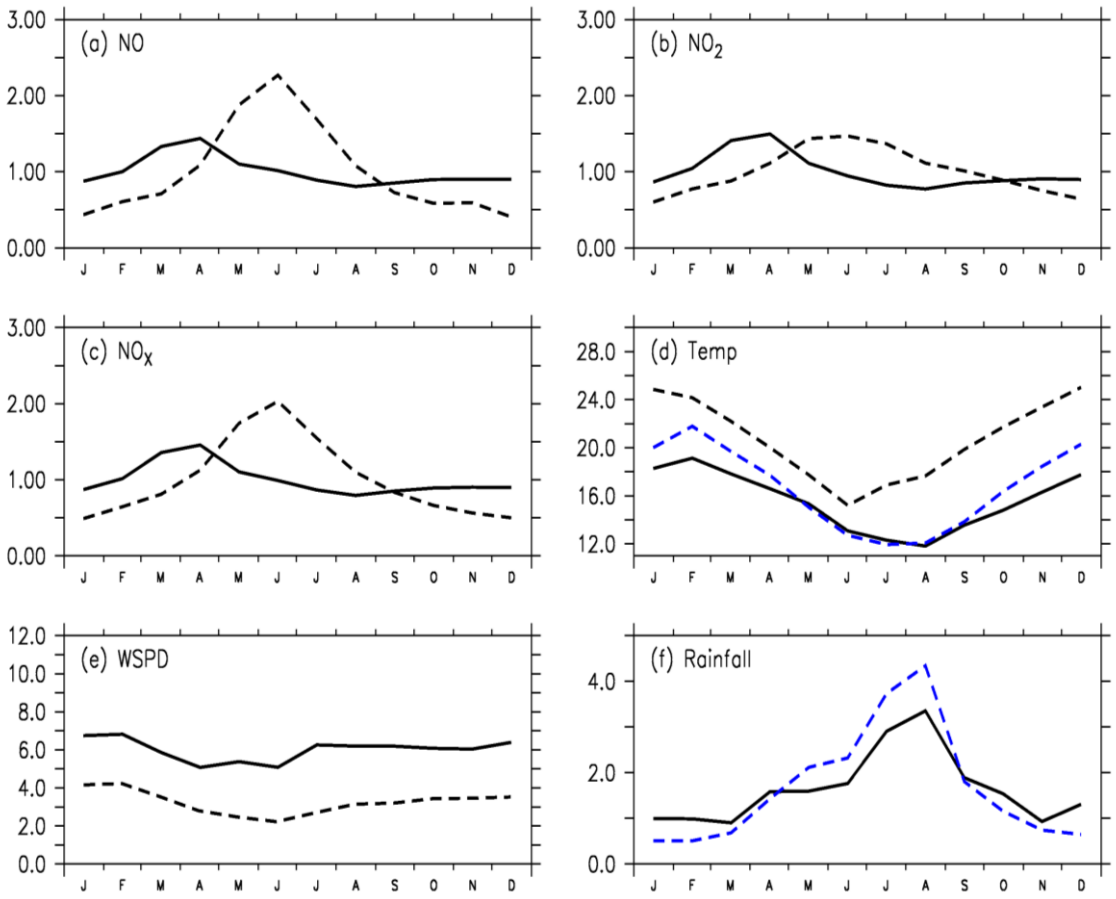

Figure 4.4: Seasonal variation of observed and simulated (a) NO (b) NO2 (c) NOx (d) Temperature (e) Wind Speed and (f) Rainfall. The station observations are in black dashes; CRU observations in blue dashes; and RegCM in a black line. The NO, NO2 and NOx are normalised with their annual mean values; Temperature is in oC, Wind Speed in m s-1; and Rainfall in mm day-1

4.3 Characteristics of the simulated pollutants and atmospheric conditions over South Africa

This section presents the RegCM simulation work and analyses performed in this research work. These analyses include the annual mean, seasonal variation, and the pollutant transports during the extreme events. These have been presented in the following sub-sections.

4.3.1 Annual mean

RegCM simulates the hot spots of NO, NO_2 and HNO_3 concentrations over the north-east South Africa (Figure 4.5). The maximum concentration of NO (about 30 x 10^{-6} g kg^{-1}) is over the Mpumalanga Highveld, an area of intense industrial activity in South Africa (Collett et al. 2010). The maximum concentration of NO_2 (about 5.0 x 10^{-6} g kg^{-1}) is also over the Mpumalanga Highveld, but the magnitude is lower than that of NO because NO_2 forms from the reaction of NO with other substances (see Eqn. 1.1); the reaction depends on the availability of those substances and on the atmospheric condition. The maximum concentration of HNO_3 (about 5.0 x 10^{-6} g kg^{-1}) is also lower than that of NO, but HNO_3 concentrations cover a wider area than those of NO and NO_2 concentrations. For instance, the contour of 0.5 x 10^{-6} g kg^{-1} in HNO_3 covers almost the entire country, but those of NO and NO_2 are limited to the eastern part of the country (Fig. 4.5). This is because most NO and NO_2 are converted to HNO_3 as they are transported away from the hotspots.

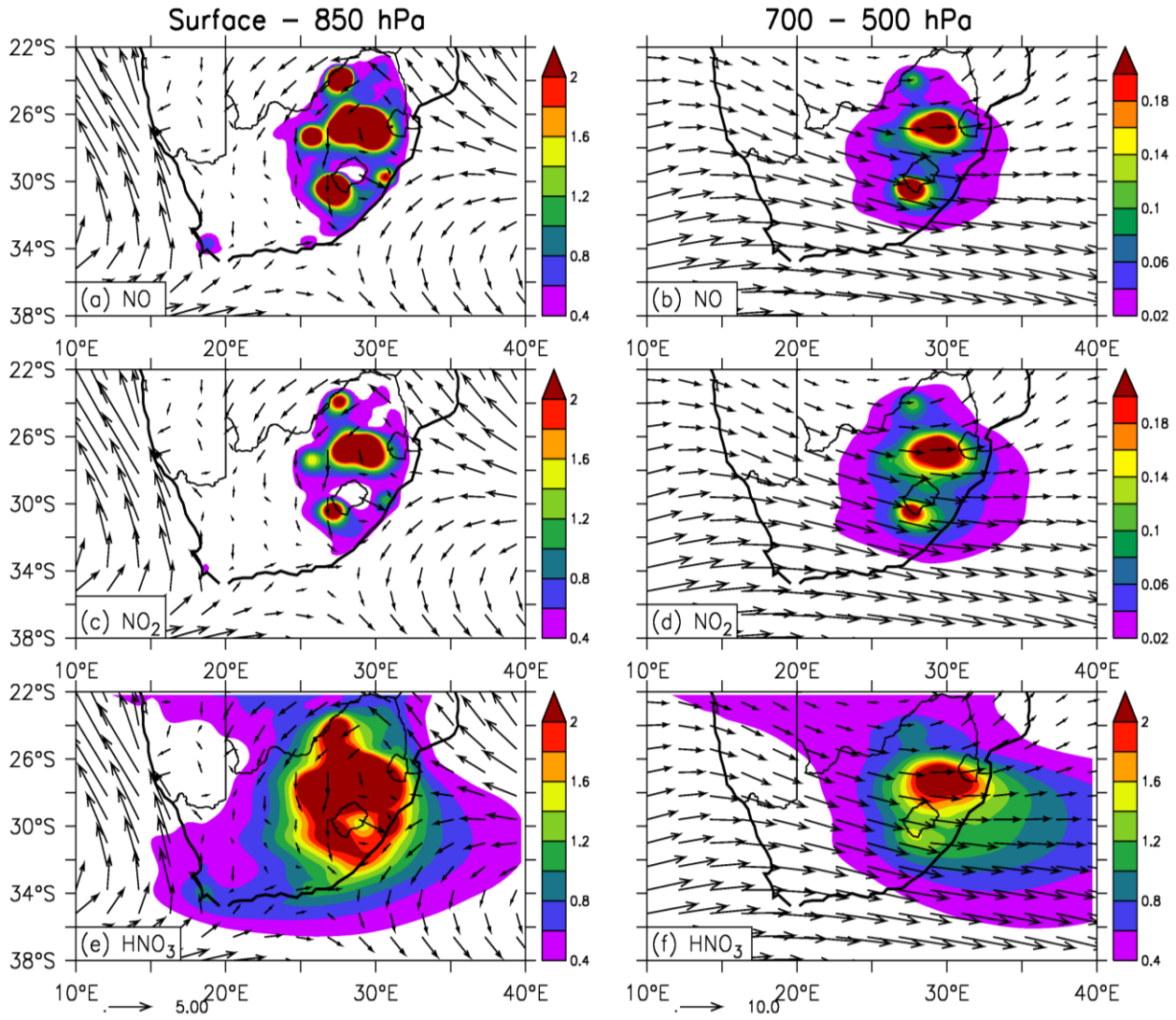

Figure 4.5: RegCM4 simulated annual mean (2001 -2004) concentration for NO (x 10^{-6} g kg^{-1}; top panels (a and b)), NO_2 (x 10^{-6} g kg^{-1}; middle panels (c and d)) and HNO_3 (x 10^{-6} g kg^{-1}; bottom panels (e and f)) at low-level (surface – 850hPa; left panels) and middle-level (700 -500 hPa; right panels) over South Africa. The corresponding wind speeds are shown with arrows; the arrows at the base of the bottom panels (e and f) show the wind scale of 5m/s and 10m/s, respectively

The model simulation shows a difference in the transport of the pollutants (NO, NO_2 and HNO_3) at low level (surface – 850 mb) and at upper level (700 – 500 mb) (Fig. 4.5). At the upper level (i.e., 700hPA), the wind pattern is dominated by a westerly flow with a weak trough over the western coast and an anti-cyclonic flow over the north-east of South Africa. At this level, the westerly flow transports most pollutants from the hot spots

towards the Indian Ocean, while the anti-cyclonic flow recycles the pollutants over South Africa. But, at low level, the wind pattern is dominated by the northerly and the north-easterly flows over the continent, the south-westerly and the south-easterly flow over the Atlantic Ocean, and the easterly flows over the Indian Ocean. The northerly and the north-easterly flows transport pollutants from the hotspots toward the southern coast and to CT. The northerly flow converges with the southerly winds along the southern coasts. The convergence produces weak winds and induces accumulation of the pollutants over the south-western half of the South Africa, along the southern coasts, and over CT. The easterly flow transports fresh air from the Indian Ocean to the eastern coast, but also picks up pollutants from the hotspots and transports them along the coastline towards the CT area. Hence, while the upper level winds (westerlies) transport fresh-air eastward from Atlantic Ocean over the CT area, the surface winds (easterlies and north-easterlies) transport pollutants from the Mpumalanga Highveld toward the city.

The emphases of previous studies have been on the eastward transport of Highveld pollutants by the upper-level westerly flow and on the recirculation of the pollutants over southern Africa by the anti-cyclones. For instance, Freiman and Piketh (2002) showed that 39% of pollutants from the Highveld are transported to the Indian Ocean, 33% are recycled over the sub-continent, while only 6% are transported by the northerly flow to the south of the Indian Ocean. But, the present results suggest that the amount of HNO_3 transported from the Highveld pollutants southward (and towards CT) may be substantial. Given that the winds are weaker at low level than at the upper level, and the pollutant concentrations are higher at low-level, it is important to have a better understanding of the pollutants transport at the low-level, especially over South Africa. In using a high resolution (about 1.5km x 1.5km) simulation over the Western Cape, Jury et al. (1990) attribute the weak wind over the Western Cape to convergence of the land and sea breezes. The present study, however, suggests that the weak wind may be due to convergence of synoptic scale flows and although the lower resolution (30km x 30km) simulation used in the present study cannot distinguish between land and sea breezes, the simulation shows that weak wind covers a wider domain than shown by Jury et al. (1990).

4.3.2 Seasonal variation

The simulated HNO_3 over South Africa exhibits a seasonal variability, in which atmospheric condition plays a major role (Fig. 4.6). The highest variability in HNO_3 occurs over the Mpumalanga Highveld, with positive anomalies from April – September, and negative anomalies from October – March. The anomalies can be attributed to the prevailing atmospheric condition during these periods. In summer (October - January), the inversion layer over the eastern coast is elevated above the mountain range (i.e., the escarpment). This allows the easterly flow from the Indian Ocean to penetrate inland and dilute the concentration of HNO_3 over the Mpumalanga Highveld (Fig. 4.7). In winter (April – August), the reverse is the case when the inversion layer is lower than the peak of the escarpment. The easterly flow cannot penetrate inland with the fresh air; instead, it deflects around the mountain ranges southward along the coastline or northward toward Mozambique. Rainfall may also lower the HNO_3 concentration in summer, because the eastern part of South Africa experiences intense rainfalls in summer and the rainfall will cleanse the atmosphere of HNO_3.

The seasonal variation of HNO_3 is weaker over Cape Town than over the Mpumalanga Highveld, but the anomalies over CT are substantial and are influenced by the transport of HNO_3 from the Mpumalanga Highveld region. The seasonal variability shows strong positive anomalies of HNO_3 from February – April, and weaker negative anomalies in the other months. The months with the positive anomalies feature easterly and north-easterly flows, transporting HNO_3 from the Mpumalanga Highveld towards CT, while the months with negative anomalies are characterised by the south-westerly, transporting fresh maritime air towards CT. The removal of HNO_3 from the atmosphere by the winter rainfall may contribute to the negative anomalies in the winter months.

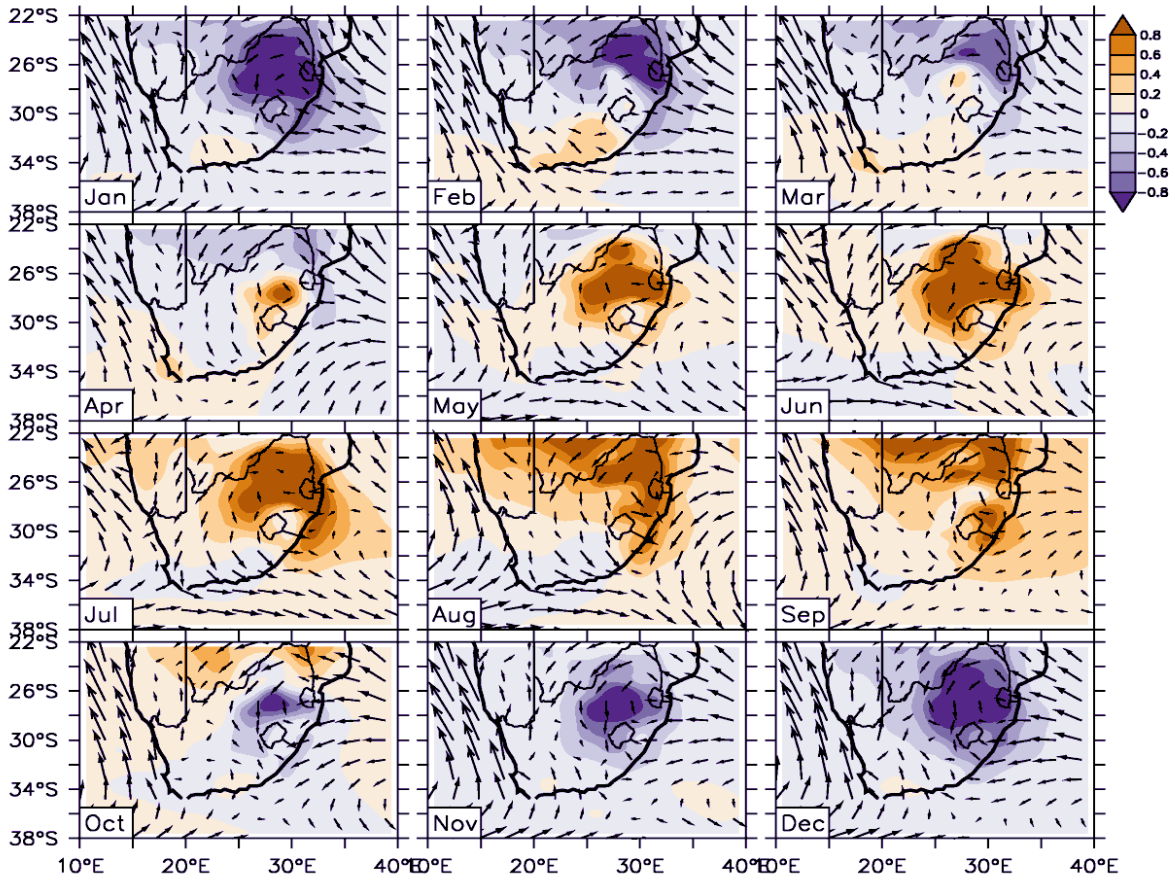

Figure 4.6: The monthly anomalies of the simulated HNO_3 concentrations (x 10^{-6} g kg^{-1}) over South Africa

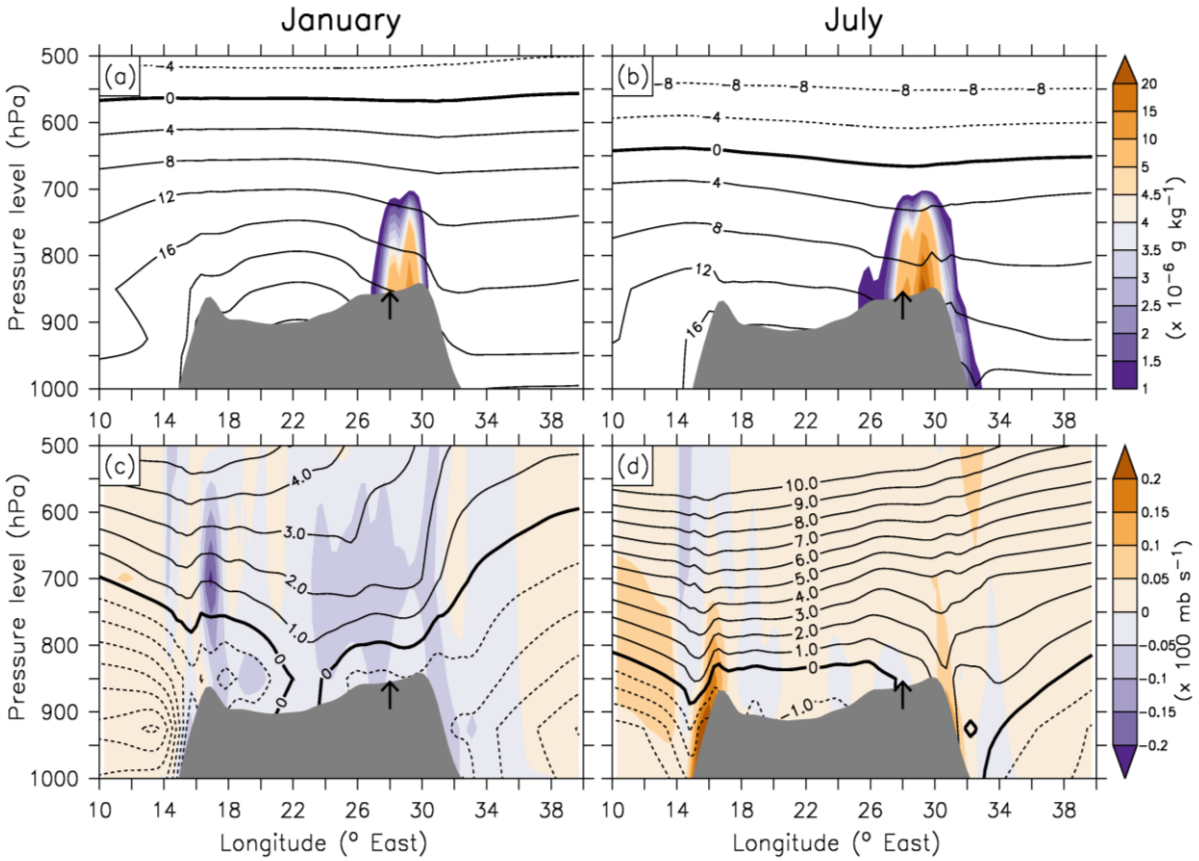

Figure 4.7: Vertical cross section of HNO_3 concentration (x 10^{-6} g kg^{-1}; shaded in upper panels (a and b) and temperature (^oC; contours in the same upper panels), vertical wind component (x 100 mb s^{-1}; shaded in lower panels (c and d), and zonal wind component (m s^{-1}; contours in the same lower panels) at latitude 26^{o}S in January and August. Topography is shown in grey colour and the location of the Highveld indicated with a black arrow (↑) on the grey background in each panel.

Table (4.1) below presents the monthly budget of the pollutants' (NO, NO_2, NO_x and HNO_3) fluxes over CT at low level. The monthly mean of the net flux is positive for all the pollutants in each month. That means that, over the city, the magnitude of outgoing pollutants is greater than the magnitude of incoming pollutants; so, Cape Town is a source for the pollutants. For all the pollutants, the maximum net flux occurs in April and the minimum in November, January, or August. The west boundary of the city always experiences outward fluxes of pollutants, except in June when it experiences inward fluxes of HNO_3 (Table 4.1); its maximum outward flux occurs in January. The north boundary features inward fluxes for the pollutants in April – August, but outward fluxes in the remaining months. The reverse is the case at the southern boundary, where there are

outward fluxes from April – August, but inward fluxes in the other months. However, in most cases, the magnitudes of the outward fluxes at the western boundary are greater than the magnitude of the outward or inward fluxes at other boundaries. Hence, Cape Town is a net exporter of pollutants, and most of the pollutants from the city are exported through the west boundary; however, as it will be shown later, the situation is different during extreme pollution events.

Table 4.1: Pollutant flux budget over Cape Town, showing the inward and outward fluxes of the pollutants (NO, NO_2, NO_x and HNO3) at the west (F_W), east (F_E), south (F_S) and north (F_N) boundaries of CT and the net flux over the city. A positive zonal flux (F_E or F_W) implies a westerly flux (i.e., flux from east of the boundary) while a negative zonal flux means the opposite. A positive meridional flux (F_N or F_S) denotes a southerly flux (i.e., flux from south of the boundary) while a negative zonal flux means the opposite. The inward fluxes are in red while the outward fluxes are in black. A positive net flux indicates divergence (i.e., depletion) of the pollutant over the city while a negative net flux indicates convergence (i.e., accumulation) of the pollutant over the city

	Jan.	Feb.	Mar.	Apr.	May	Jun.	Jul.	Aug.	Sept.	Oct.	Nov.	Dec.
NO												
F_W	-1.9	-2.4	-2.2	-1.3	-0.6	0.0	-0.4	-0.3	-1.1	-1.1	-1.6	-1.7
F_E	-0.4	-1.0	-0.8	0.3	0.5	0.9	0.6	0.9	0.2	0.2	-0.2	-0.4
F_S	1.6	1.5	1.5	-0.4	-0.7	-1.5	-1.2	-0.6	0.3	0.4	1.5	1.4
F_N	1.2	1.0	1.6	-0.2	-0.3	-0.7	-0.6	-0.3	0.1	0.4	1.0	1.2
Net Flux	**1.1**	**0.9**	**1.5**	**1.7**	**1.5**	**1.7**	**1.6**	**1.5**	**1.2**	**1.3**	**0.9**	**1.0**
NO2												
F_W	-1.5	-2.0	-1.8	-1.0	-0.5	0.0	-0.4	-0.3	-0.9	-0.9	-1.3	-1.4
F_E	-0.3	-0.6	-0.4	0.2	0.3	0.5	0.3	0.4	0.0	0.1	-0.2	-0.2
F_S	1.2	1.2	1.2	-0.3	-0.5	-1.0	-0.7	-0.4	0.2	0.3	1.1	1.0
F_N	0.8	0.8	1.0	-0.1	-0.2	-0.4	-0.4	-0.2	0.1	0.3	0.7	0.8
Net Flux	**0.9**	**1.0**	**1.2**	**1.4**	**1.1**	**1.0**	**1.0**	**0.9**	**0.8**	**1.0**	**0.8**	**0.8**
NOX												
F_W	-3.4	-4.4	-4.0	-2.2	-1.1	-0.1	-0.8	-0.6	-2.0	-2.0	-2.9	-3.0
F_E	-0.7	-1.5	-1.2	0.5	0.8	1.3	1.0	1.3	0.2	0.2	-0.4	-0.6
F_S	2.8	2.7	2.7	-0.7	-1.2	-2.5	-1.9	-1.0	0.5	0.6	2.5	2.5
F_N	1.9	1.8	2.6	-0.3	-0.6	-1.1	-1.0	-0.5	0.2	0.6	1.7	1.9
Net Flux	**1.9**	**1.9**	**2.7**	**3.1**	**2.6**	**2.8**	**2.6**	**2.3**	**2.0**	**2.2**	**1.7**	**1.9**
HNO3												
F_W	-3.1	-4.7	-3.7	-1.5	-0.8	0.2	-0.6	-0.5	-2.2	-1.6	-2.6	-2.8
F_E	-1.7	-3.0	-1.6	0.0	0.0	0.6	0.0	0.2	-1.2	-0.7	-1.1	-1.5
F_S	2.8	3.4	3.0	-0.4	-0.7	-1.7	-1.6	-0.7	0.7	0.7	2.5	2.6
F_N	1.8	2.1	2.2	-0.3	-0.6	-1.2	-1.7	-0.6	0.0	0.4	1.6	1.7
Net Flux	**0.4**	**0.4**	**1.2**	**1.6**	**1.0**	**0.9**	**0.6**	**0.8**	**0.4**	**0.6**	**0.5**	**0.4**

4.3.3 Transport of pollutants during extreme events in Cape Town

The time series of the simulated pollutants' concentration over Cape Town (see Fig. 4.8 below) shows that the extreme concentration events (defined as 99 percentiles; ≥ 3.3 x 10^{-6} g kg^{-1} for NO_x; ≥ 2.8 x 10^{-6} g kg^{-1} for HNO_3) mostly occur in April. With respect to NO_x (see Fig. 4.8c), the extreme events occurred once in 2001, but twice in 2003 and 2004. For HNO_3, the extreme events occurred once 2001, three times in 2002 and twice in 2003 and 2004. However, the extreme events for NO_x and HNO_3 rarely occur on the same day, suggesting that, in Cape Town the atmospheric conditions that induce NO_x extreme events may be different from those that induce HNO_3 extreme events.

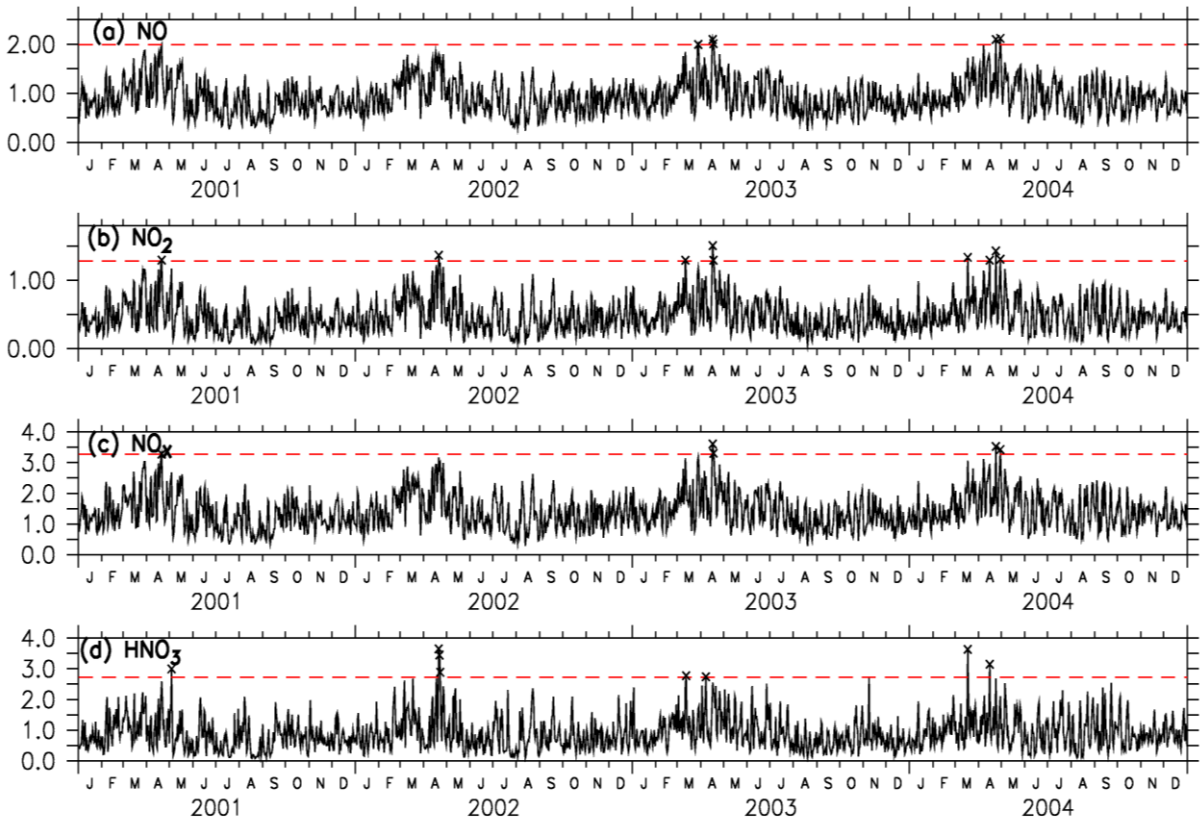

Figure 4.8: The time series of the simulated pollutants' concentration over Cape Town in 2001 – 2004. The extreme values (99 percentiles) are indicated with red dashes.

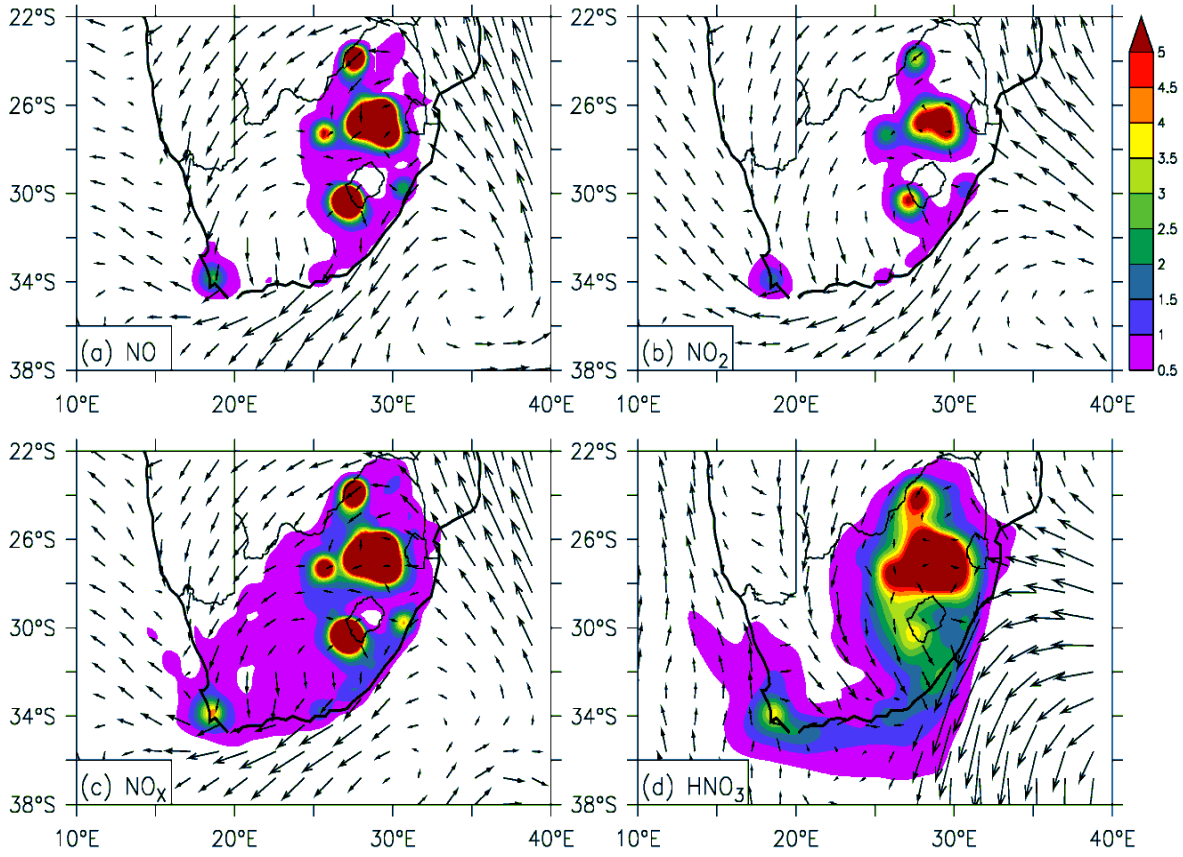

Figure 4.9: The composite of low-level (surface – 850hPa) wind flow (arrows) during the extreme pollution events in CT. The corresponding pollutants' concentration (NO, NO2, NOx and HNO3; x 10^{-6} g kg^{-1}) are shaded.

The composite of wind flow during extreme pollution events in CT shows a transport of pollutants from the Mpumalanga Highveld to Cape Town at surface (Fig. 4.9). For NO_x extreme events, the low-level wind pattern is characterised with the northerly and the north-easterly flows, transporting the pollutant from the Mpumalanga Highveld towards CT and its south coast. Along the south coastline, there is a confluence of the northerly flow and the easterly flow, and the easterly flow also transports pollutants from the eastern part of South Africa towards CT. The wind pattern also features a col over Cape Town. A col is a relatively neutral area of low pressure between two anti-cyclones, or a point of intersection of a trough (in cyclonic flow) and a ridge (in anti-cyclonic flow). It is usually associated with a calm or light variable wind, which causes stagnation of air flow. Since a col can cause the accumulation of atmospheric pollution (Stein et al 2003), the formation of a col with the convergence of the north-easterly and the southerly over CT will provide a favourable atmospheric condition for the accumulation of pollutants over

the city during the extreme events. At 700hPa (Fig. 4.10 below), there is a strong anti-cyclonic flow over the southern Africa. This anti-cyclone will produce a strong subsidence over South Africa, and the subsidence will prevent a vertical mixing of the pollutants, capping the high concentrations of pollutants close to the surface as they are transported from the Mpumalanga Highveld toward Cape Town.

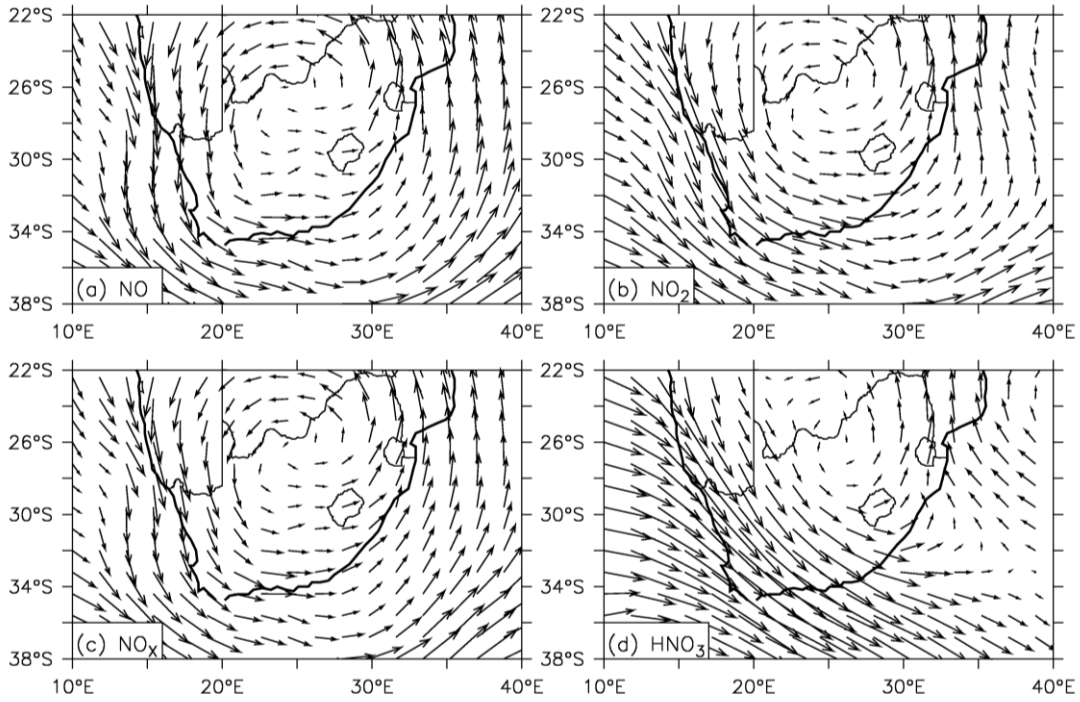

Figure 4.10: The composite of 700hPa wind during extreme events of pollutants' (NO, NO2, NOx and HNO3) concentration at surface in Cape Town.

The synoptic wind patterns that induce the extreme HNO_3 events differ from those that induce the extreme NO_x events (Figure 4.9d) With the HNO_3 extreme events, the low-level wind pattern features a strong north-westerly flow, transporting HNO_3 from the Mpumalanga Highveld towards the south coast. In addition, it shows a strong easterly flow transporting fresh air from the Indian Ocean, but turns poleward as it approaches the escarpment. This deflects the fresh air from the continent and at the same time forms a confluence flow with the north-westerly flow along the coast.

The wind patterns also feature a weak wind pattern along the south coast, and a col over CT. Hence, there is a band of high HNO_3 concentration along the coast that, links the peak HNO_3 concentration at Cape Town with the one over the Mpumalanga Highveld. As

with NO_x extreme events, the 700hPa wind pattern features a strong anti-cyclone (centering over the border between South Africa and Botswana) but with a stronger north-westerly flow over the western flank of South Africa.

Table 4.2 below shows that Cape Town is a sink for all the pollutants during the extreme events, except for HNO_3 in March and April. For NO_x (NO and NO_2), while the west boundary experiences outward fluxes, the east and north boundaries experience inward fluxes with higher magnitudes than the outward fluxes at the west boundary. The directions of the fluxes at the south boundary vary: inward fluxes for NO in March, NO_2 in March and April, but outward fluxes for NO and NO_x in April. Nevertheless, net fluxes for NO_x (NO and NO_2) are negative, meaning an accumulation of NO_x (NO and NO_2) over the city, during the extreme events. The characteristics of HNO_3 fluxes during the extreme events differ from (and are more complex than) that of NO_x. For HNO_3, the west and north boundaries experience inward fluxes during the extreme events in March and May, but outward fluxes in April. The east boundary experiences outward fluxes of HNO_3, while the south boundary experiences inward fluxes in April, but outward fluxes in March and May. Nevertheless, the table indicates an accumulation of HNO_3 over CT in May, though not in March and April.

Table 4.2: The low-level fluxes of pollutants (NO, NO2, NOx and HNO3) at west, east, south and north boundaries in Cape Town during the extreme event. A positive zonal flux (F_E or F_W) implies a westerly pollutant flux (i.e., pollutant flux from east of the boundary) while a negative zonal flux means the opposite. A positive meridional flux (F_N or F_S) denotes a southerly pollutant flux (i.e., pollutant flux from south of the boundary) while a negative zonal flux means the opposite. The inward fluxes into CT are in red while the outward fluxes from CT are in black. A positive net flux indicates divergence (i.e., depletion) of the pollutant over the city while a negative net flux indicates convergence (i.e., accumulation) of the pollutant over the city.

	NO		**NO_2**		**NO_X**	**HNO_3**		
	March	April	March	April	April	March	April	May
F_W	-3.1	-0.4	-0.9	-1.0	-0.7	1.4	-0.5	1.0
F_E	-3.0	-0.7	-0.5	-0.9	-1.4	1.3	0.7	1.1
F_S	0.8	-0.9	0.5	0.1	-0.8	-0.8	1.8	-0.6
F_N	-1.1	-2.0	-0.6	-1.1	-1.6	-0.4	0.8	-1.0
Net Flux	**-1.8**	**-1.3**	**-0.7**	**-1.1**	**-1.4**	**0.3**	**0.2**	**-0.3**

Chapter Five: Conclusion and recommendations

5.0 Summary

As part of the ongoing efforts to understand the sources of pollution in Cape Town, this study has applied a RegCM to study the transport of NO_x and HNO_3 over Africa, with emphasis on the pollutants' transport from the Mpumalanga Highveld to Cape Town. It also examined whether Cape Town is a net sink or source for pollutants.

The model accounts for the influence of southern African complex topography, atmospheric conditions and the pollutants' chemical reactions in simulating the emission, dispersion and transport of these pollutants. The study (i) described the characteristics of observed NO and NO_2 over Cape Town, (ii) examined how well the regional model captures the characteristics, and (iii) analysed the model simulations to describe the influence of atmospheric conditions on the seasonal variations of pollutants over South Africa. It also (iv) calculated the flux budget of pollutants over the city for each month and for composite of days with extreme pollution events.

The diurnal variation of NO_x over Cape Town exhibits two peaks (a morning and an evening peak) mainly due to traffic rush, but the atmospheric conditions also play a critical role in the morning peak. The seasonal variations are more influenced by changes in the atmospheric conditions than changes in the local emissions from traffic or industry. The model captures the seasonal variations of NO_x (NO and NO_2) concentrations as observed, except that it underestimates the anomalies from May – June. The correlation coefficient between the observed and simulated daily concentrations of the pollutants is about 0.4, while the normalised standard deviation varies between 0.4 and 1.0; the model performs better in simulating the atmospheric variables.

While the results of this study agree with those from previous studies that the Mpumalanga Highveld's pollutants are transported eastward by the westerly flow at 700hPa, it shows that this is reversed at low-level (surface – 850 hPa) where the concentration of pollutants is higher. At low-level, the easterly and the north-easterly flows transport the Mpumalanga Highveld's pollutants westward toward Cape Town. During the extreme events, however, the north-easterly flow transports NO_x directly from the Mpumalanga Highveld to Cape Town; a band of high concentration of HNO3 links the

peak HNO_3 concentration at CT with that of Mpumalanga Highveld, and the 700hPa synoptic wind features a strong anti-cyclone that induces strong subsidence over South Africa. The formation of smog over Cape Town, during extreme events, makes the city conducive for the accumulation of pollutants. However, the pollutants' budget flux over Cape Town shows that the city could be a net source or net sink for NO_x and HNO_3 during extreme events.

Since these results are based on four years simulation from one model, there is need for longer simulations with multi-models to establish the robustness of the findings. A longer simulation will account for the influence of inter-annual variability on the results, while using multi-model simulations will provide opportunity for model comparisons and for assessing the degree of inter-model variability. However, the present study suggests that the transport of NO_x and HNO_3 from the Mpumalanga Highveld may contribute to the pollutants' concentration in Cape Town.

5.1 Publication(s)

Abiodun, B. J., Ojumu, A. M., Jenner, S. & Ojumu, T. V. 2012. Transport of atmospheric NO_x and HNO_3 over Cape Town. *Atmospheric Chemistry and Physics*. 11827-11862. (Accepted and published as a discussion paper).

References

Abiodun, BJ, Enger, L. 2002. The role of advection of fluxes in modelling dispersion in convective boundary layers. *Quarterly Journal of the Royal Meteorological Society* 128(583):1589-1607.

allAfrica. 2008. South Africa: Cape Town unveils air pollution awareness campaign. Available at: http://allafrica.com/stories/200804100298.html?maneref=http%3A%2F%2Fwww.google.co.uk%2Fsearch%3Fhl&3Den%26tbm%3D%26ie%3DUTF-8%26q%3DCape%2Btown%2Bair%2Bquality%2Bguidelines%253A%2Ball%2Bafrica.com%2B&mstac=0 (accessed on 02/10/2010).

Anthes, RA. 1977. A cumulus parameterization scheme utilizing a one-dimensional cloud model. *Mon. Wea. Rev.* 105:270–286.

Andr´en (1987:1045-1058)

CCT. 2001. City of Cape Town air pollution control by-law. Available at: http://www.westerncape.gov.za/text/2006/4/air_pollution_by-law.pdf (Accessed on 21/05/2013).

CCT. 2005. *Final report on air quality management plan for the City of Cape Town*. In Town, CC. (ed). Report AQM 20050823 - 001.

Chameides, WL, Lindsay, RW, Richardson, J & Kiang CS. 1988. The role of biogenic hydrocarbons in urban photochemical smog: Atlanta as a case study. *Science* 241(4872):1473-1475.

Collett, KS, Piketh, SJ & Ross, KE. 2010. An assessment of the atmospheric nitrogen budget on the South African Highveld. *South African Journal of Science* 106(5/6): 1–9.

Collins, WD, Bitz, CM, Blackmon, ML, Bonan, GB, Bretherton, CS, Carton, JA, Chang, P, Doney, SC, Hack, JJ, Henderson, TB, Kiehl, JT, Large, WG, Mckenna, DS, Santer, BD & Smith, RD. 2006. The Community Climate System Model version 3 (CCSM3). *Journal of Climate* 19:2122–2143.

Climate Research Unit. 2012. Available at: http://www.cru.uea.ac.uk/data (Accessed on 01/08/2012).

Dean, SW. 1990. Corrosion testing of metals under natural atmospheric conditions (STP 1000). In *Corrosion Testing and Evaluation, Silver Anniversary Volume*. Philadelphia: ASTM.

Deardoff, JW. 1978. Efficient prediction of ground surface temperature and moisture with inclusion of a layer of vegetation. *Journal of Geophysical. Resesearch* 83:1889–1903.

Dickinson, RE. 1984. *Modeling evapotranspiration for three-dimensional global climate models*. In Hansen JE & Takahashi, T (eds). Climate Processes and Climate Sensitivity. Washington: American Geophysical Union.

Dickinson, RE, Kennedy, PJ, Henderson-Sellers, A & Wilson, M. 1986. Biosphere-atmosphere transfer scheme (bats) for the ncar community climate model. Technical Report, NCARE/TN-275+STR, National Center for Atmospheric Research.

Dickinson, RE, Errico, RM, Giorgi, F & Bates, GT. 1989. A regional climate model for the western United States. *Climatic Change* 15:383–422.

Dickinson, RE, Henderson-Sellers, A & Kennedy, PJ. 1993. *Biosphere-atmosphere transfer scheme (BATS) version 1e as coupled to the NCAR community climate model*. NCAR Technical report, NACR, Boulder.

Egan, BA. 1984. Transport and diffusion in complex terrain (review). *Boundary-Layer Met.* 30:3-28.

Elguindi, N, Bi, X, Giorgi, F, Nagarajan, B, Pal, J, Solmon, F, Rauscher, S & Zakey, A. 2010. RegCM Version 4.0 User's Guide. Trieste, Italy.

Emanuel, KA. 1991. A scheme for representing cumulus convection in large-scale models. *Journal of Atmospheric Science* 48(21):2313–2335.

Emanuel, KA & Zivkovic-Rothman, M. 1999. Development and evaluation of a convection scheme for use in climate models, *Journal of Atmospheric Science* 56:1766–1782.

Emmons, LK, Walters, S, Hess, PG, Lamarque, JF, Pfister, GG, Fillmore, D, Granier, C, Guenther, A, Kinnison, D, Laepple, T, Orlando, J, Tie, X, Tyndall, G, Wiedinmyer,C, Baughcum, SL & Kloster, S. 2010. Description and evaluation of the model for ozone and related chemical tracers, Version 4 (MOZART-4). *Geoscientific Model Development* (3):43–46.

Enger, L. 1986. A higher order closure model applied to dispersion in a convective PBL. *Atmospheric Environment* 20:879-894.

Enger, L. 1990a. Simulation of dispersion in moderately complex terrain-Part A. The fluid dynamic model. *Atmospheric Environment* 24:2431-2446.

Enger, L. (1990b) Simulation of dispersion in moderately complex terrain-Part B. The higher order closure dispersion model. *Atmospheric Environment* 24:2447-2455.

Enger, L & Koracin D. 1995. Simulation of dispersion in complex terrain using a higher-order closure model. *Atmospheric Environment* 29:2449-2465.

Fields, S. 2004. Cycling out of Control. *Environmental Health Perspectives* 112(10): 556–563.

Fitzpatrick, T. 2006. Effects of air pollution on your health. Available at: http://environmentalchemistry.com/yogi/environmental/200602airpollution.html (Accessed on 08/03/2011).

Freiman, MT & Piketh, SJ. 2003. Air transport into and out of the industrial Highveld region of South Africa. *Journal of Applied Meteorology* 42(7):994–1002.

Fritsch, J.M. & Chappell, C.F., 1980. Numerical prediction of convectively driven mesoscale pressure systems, Part I: Convective parameterization. *Journal of Atmospheric Science*, 37, 1722–1733.

Giorgi, F. & Bates, G. T. 1989. The climatological skill of a regional model over complex terrain. *Mon. Weather Rev*. 117:2325–2347.

Giorgi, F.1990. Simulation of regional climate using a limited area model nested in a general circulation model, *Journal of Climate* 3:941–963.

Giorgi, F & Marinucci, MR. 1991. Validation of a regional atmospheric model over europe: Sensitivity of wintertime and summertime simulations to selected physics parameterizations and lower boundary conditions. *Quarterly Journal of the Royal Meteorological Society* 117:1171–1206.

Giorgi, F, Anyah, RO & Bates, GT. 1993. Development of a second-generation Regional Climate Model (RegCEM2): part I: boundary-layer and radiative transfer processes. *National Center for Atmospheric Research* 121:2794–2812.

Giorgi, F, Bi X & Qian, Y. 2002. Direct radiative forcing and regional climatic effects of anthropogenic aerosols over East Asia: a regional coupled climate/chemistry-aerosol model study. *Journal of Geophysical Research* 107:4439.

Giorgi, F & Anyah, RO. 2012a. The Road Towards RegCM4. *Climate Research*. 52:3–6.

Giorgi, F, Coppola, E, Solmon, F, Mariotti, L, Sylla, MB, Bi, X, Elguindi, N, Diro, GT, Nair, V, Giuliani, G, Turuncoglu, UU, Cozzini, S, Güttler, I, O'Brien, TA, Tawfik, AB,

Shalaby, A, Zakey, AS, Steiner, AL, Stordal, F, Sloan, LC, Bran, C. 2012b. RegCM4: model description and preliminary tests over multiple CORDEX domains. *Climate Research* 52:7-29.

Greater Johannesburg Metropolitan Council. 2000. Impact of air pollutant. Available at: http://www.ceroi.net/reports/johannesburg/csoe/html/nonjava/Pollution/Air/impact.htm (Accessed on 08/03/ 2011).

Grell, G. 1993. Prognostic evaluation of assumptions used by cumulus parameterizations. *Mon.Wea. Rev.* 121:764–787.

Grell, GA, Dudhia, J & Stauffer, DR. 1994. Description of the fifth generation Penn State/NCAR Mesoscale Model (MM5), Technical Report, TN-398+STR, NCAR, Boulder, Colorado.

Grell, GA, Peckhama, SE, Schmitzc, R, McKeenb, SA, Frostb, G, Skamarockd, WC & Eder B. 2005. Fully coupled online chemistry within the WRF model. *Atmospheric Environment* 39:6957–6975.

Guenther, A, Karl, T, Harley, P, Wiedinmyer, C, Palmer, PI & Geron, C. 2006. Estimates of global terrestrial isoprene emissions using MEGAN (Model of Emissions of Gases and Aerosols from Nature). *Atmospheric Chemistry and Physics* 6:3181–3210.

Holtslag, AAM, De Bruijn, EIF & Pan, HL. 1990. A High Resolution Air Mass Transformation Model for Short-Range Weather Forecasting. *Monthly Weather Review* 118:1561-1575.

Holtslag, AAM & Boville, BA. 1993. Local versus nonlocal boundary-layer diffusion in a global climate model. *Journal of Climate* 6:1825–1842.

Hunt, JCR, Puttok, JS & Snyder, WH. 1979. Turbulent diffusion from a point source in stratified and neutral flows around a three-dimensional hill-I. Diffusion equation analysis. *Atmospheric Environment* 13:1227-1239.

Jacobson, MZ. 2002. *Atmospheric Pollution History, Science, and Regulation*. Cambridge: Cambridge University Press.

Jenner, SL. 2013. The transport of pollutants over South Africa and atmospheric sulphur in Cape Town. M.P.h. Thesis, University of Cape Town, Cape Town.

Jury, M, Tegen, A, Ngeleza, E & Dutoit, M. 1990. Winter air-pollution episodes over Cape-Town. *Boundary-Layer Meteorology* 53**:**1-20.

Kalognomou, EA. 2009. Air quality and climate change in the greater Cape Town area. *Environmental and Geographical Science.* M.Sc. Thesis, University of Cape Town, Cape Town.

Kiehl, JT, Hack, JJ, Bonan, GB, Boville, BA, Brigleb, BP, Williamson, DL & Rasch, PJ. 1996. *Description of the NCAR community climate model (CCM3),* Technical report, NCAR, Boulder.

Kok, JF. 2011. A scaling theory for the size distribution of emitted dust aerosols suggests climate models underestimate the size of the global dust cycle. *Proc Natl Acad Sci USA* 108:1016–1021.

Konare, A, Zakey, AS, Solmon, F, Giorgi, F, Rauscher, S, Ibrah, S & Bi, X. 2008. A regional climate modeling study of the effect of desert dust on the west African monsoon. *Journal of Geophysical Research* 113(D12).

Lamb, RG. 1979. The effects of release height on material dispersion in the convective planetary layer. Preprint vol. Amer. Meteor. Soc. *Fourth Symposium on Turbulence, diffusion and Air Pollution*, Reno, N.V.

Laurent, B, Marticorena, B, Bergametti, G, Leon, JF & Maho -wald, NM. 2008. Modeling mineral dust emissions from the Sahara desert using new surface properties and soil database. *Journal of Geophysical Research* 113(D14).

Lawrence, P & Chase, T. 2007. Representing a new MODIS consistent land surface in the Community Land Model (CLM3.0). *Journal of Geophysical Research* 112(GI):1-27.

Linde, H & Ravenscroft, G. 2003. Air quality management in the City of Cape Town.

Madronich, S & Flocke, S. 1999. The role of solar radiation in atmospheric chemistry. In P. Boule (eds). New York: Handbook of Environmental Chemistry, Springer-Verlag.

Malavelle, F, Pont, V, Mallet, M, Solmon, F, Johnson, B, Leon, JF & Liousse, C. 2011. Simulation of aerosol radiative effects over West Africa during DABEX and AMMA SOP-0. *Journal of Geophysical Research* 116(D08).

Mauderly, JL & Samet, JM. 2009. Is there evidence for synergy among air pollutants in causing health effects?. *Environmental Health Perspectives* 117**:**1-6.

Maynard, AD & Maynard, RL. 2002. A derived association between ambient aerosol surface area and excess mortality using historic time series data. *Atmospheric Environment* 36**:**5561-5567.

Misra, PK. 1980. Dispersion from tall stacks into a shoreline environment, *Atmospheric Environment* 14:397-400

Mitchell, TD & Jones, PD. 2005. An Improved Method of Constructing a Database of Monthly Climate Observations and Associated High-resolution grids. *International Journal of Climatology* 25:693-712.

Monin, AS & Obukhov, AM. 1954. Osnovnye zakonomernosti turbulentnogo peremesivanija v prizemnom sloe atmosfery y (Basic laws of turbulent mixing in the atmosphere near the ground). *Trudy Institute Geologicheskikh Geofizi*, 24(151):163–187.

Muchapondwa, E. 2010. A cost effectiveness analysis of options for reducing pollution in Khayelitsha township, South Africa. *The Journal for Transdisciplinary Research in Southern Africa* 6(2):333-358.

Norman, R, Cairncross, E, Witi, J & Bradshaw, D. 2007. Estimating the burden of disease attributable to urban outdoor air pollution in South Africa in 2000. *South African Medical Journal* 97**:**782-790.

Oleson, K., Y. Dai, G.B. Bonan, M. Bosilovichm, R. Dickinson, P. Dirmeyer, F. Hoffman, P. Houser, S. Levis, G.-Y. Niu, P. Thornton, M. Vertenstein, Z.- . Yang, and X. Zeng,

Oleson, KW, Dai, Y, Bonan, G, Bosilovich, M, Dickinson, R, Dirmeyer, P, Hoffman, F, Houser, P, Levis, S, Niu, GY, Thornton, P, Vertenstein, M, Yang, Z & Zeng, X. 2004. Technical description of the Community Land Model. Technical Note, NCAR, Boulder.

Pal, JS, Giorgi, F, Bi, X, Elguindi, N, Solmon, F, Gao, X, Rauscher, SA, Francisco, R, Zakey, A, Winter, J, Ashfaq, M, Syed FS, Bell, JL, Diffenbaugh, NS, Karmacharya, J, Konaré, A, Martinez, D, da Rocha, RP, Sloan LC & Steiner, A. 2007. Regional Climate Modeling for the Developing World: The ICTP RegCM3 and RegCNET. *Bulletin of the American Meteorological Society* 88(9):1395–1409.

Piketh, SJ, Swap, RJ, Maenhaut, W, Annegarn, HJ, Formenti, P. 2002. Chemical evidence of long-range atmospheric transport over southern Africa. *Journal of Geophysical Research* 107(D24):1–13.

Preston-Whyte, RA, Diab, RD & Tyson, PD. 1977. Towards an inversion climatology of southern Africa, II, Non-surface inversions in the lower atmosphere. *South African Geographical Journal* 59(1):47–59.

Santese, M, Perrone, MR, Zakey, AS, De Tomasi, F & Giorgi, F. 2010. Modeling of Saharan dust outbreaks over the Mediterranean by RegCM3: case studies. *Atmospheric Chemistry and Physic*s 10:133–156.

Segal, M, McNider, RT, Pielke, RA & McDougal, DS. 1982. A numerical model simulation of the regional air pollution meteorology of the Greater Chesapeake Bay area- summer day case study. *Atmospheric Environment* 16:1381-1397.

Seinfeld, JH & Pandis, SN. 2006. *Atmospheric chemistry and physics - from air pollution to climate change*. 2nd edition. [Sl]: John Wiley & Sons.

Shalaby, AK, Zakey, AS, Tawfik, AB, Solmon, F, Giorgi, F, Stordal, F, Sillman, S, Zaveri, R.A & Steiner, AL. 2012. Implementation and evaluation of online gas-phase chemistry within a regional climate model (RegCM-CHEM4). *Geoscientific Model Development* 5:149–198.

Sillman, S, Logan, JA & Wofsy SC. 1990. The sensitivity of ozone to nitrogen oxides and hydrocarbons in regional ozone episodes. *Journal of Geophysics* 95(D2):1837-1851.

Slingo et al (1989)

Smith, SN & Mueller, SF. 2010. Modeling natural emissions in the community multiscale air quality (CMAQ) model–I: building an emissions data base. *Atmospheric Chemistry and Physics* 10**:**4931–4952.

Solmon, F, Giorgi, F & Liousse, C. 2006. Aerosol modeling for regional climate studies: application to anthropogenic particles and evaluation over a European/African domain. *Tellus Ser B Chem Phys Meterol* 58:51–72.

Solmon, F, Mallet, M, Elguindi, N, Giorgi, F, Zakey, A & Konaré, A. 2008. Dust aerosol impact on regional precipitation over western Africa, mechanisms and sensitivity to absorption properties. *Geophysical Research Letter* 35(24):1-6.

Stein, DC, Swap, RJ, Greco, S, Piketh, SJ., Macko, SA., Doddridge, BG., Elias, T & Bruintjes, RT. 2003. Haze Layer Characterization and Associated Meteorological Controls Along the Eastern Coastal Region of Southern Africa. *Journal of Geophysical Research*108 (D13):1–11.

Sundqvist, H, Berge, E & Kristjansson, JE. 1989. The effects of domain choice on summer precipitation simulation and sensitivity in a regional climate model. *Journal of Climate* 11:2698–2712.

Sylla, MB, Coppola E, Mariotti, L, Giorgi, F, Ruti, PM, Dell'Aquila, A & Bi,X. 2009. Multiyear simulation of the African climate using a regional climate model

(RegCM3) with the high resolution ERA-interim reanalysis. *Climate Dynamics* 35(1):231–247.

Tamm, CO. 1976. Acid precipitation: biological effects in soil and on forest vegetation. *Ambio* 5**:**235 - 238.

Trainer, M, Willaims, EJ, Parrish, DD, Buhr, MP, Allwine, EJ, Westberg, HH, Fehsenfeld, FC & Liu SC. 1987. Models and observation of the impact of natural hydrocarbons on rural ozone. *Nature* 329:705.

Tummon, F, Solmon, F, Liousse, C & Tadross, M. 2010. Simulation of the direct and semidirect aerosol effects on the southern Africa regional climate during the biomass burning season. *Journal of Geophysical Research* 115(D19).

Uliasz, M (eds). 1994. *Lagrangian particle modeling in mesoscale applications. Environmental Modeling II.* P. Zannetti, Computational Mechanics Publications, 71-102.

Van der Merwe, NM. 1998. Mesoscale dispersion modelling of SO2 over the South African Highveld. Ujdigispace. M.Sc. Thesis, Rand Afrikaans University, Johannesburg.

Van Tienhoven, A.M., 1999. Status of air pollution in South Africa. Available at: www.naca.org.za (accessed on 22/05/2013).

Walton, NM. 2005. Characterisation of Cape Town Brown Haze. M.Sc. Thesis, University of the Witwatersrand, Johannesburg.

Wesley, ML. 1989. Parameterization of surface resistance to gaseous dry deposition in regional-scale numerical models. *Atmospheric Environment* 23:1293–1304.

Wicking-Baird, MC., De Villiers, MG & Dutkiewicz, RK. 1997. *Cape Town Brown haze study*. Cape Town, Energy Research Institute, University of Cape Town.

White, N, te WaterNaude, J, van der Walt, A, Ravenscroft, G, Roberts, W & Ehrlich, R. 2009. Meteorologically estimated exposure but not distance predicts asthma symptoms in schoolchildren in the environs of a petrochemical refinery: a cross-section. *Environmental Health* 8:45-55.

WHO. 2003. Health aspects of air pollution with particulate matter, ozone and nitrogen dioxide. Report on a WHO Working Group, World Health Organization, Regional Office for Europe, Copenhagen.

Zakey, AS, Solmon, F & Giorgi, F. 2006. Implementation and testing of a desert dust module in a regional climate model. *Atmospheric Chemistry and Physics* 6:4687–4704.

Zakey, AS, Giorgi, F & Bi, X. 2008. Modeling of sea salt in a regional climate model: fluxes and radiative forcing. *Journal of Geophysical Research* 113(D14).

Zaveri, RA & Peters, LK. 1999. A new lumped structure photochemical mechanism for long-scale applications. Journal of Geophysical Research 30:387–415.

Zhang, L, Brook, JR & Vet, R. 2003. A revised parameterization for gaseous dry deposition in air-quality models. *Atmosmospheric Chemistry and Physics* 3:2067–2082.

Zhang, D, Zakey, AS, Gao, X, Giorgi, F & Solmon F. 2009. Simulation of dust aerosol and its regional feedbacks over East Asia using a regional climate model. *Atmospheric Chemistry and Physics* 9:1095–1110

Zunckel, M, Venjonoka, K, Pienaar, JJ, Brunke, EG, Pretorius, O, Koosialee, A, Raghunandan, A & Van tienhoven, AM. 2004a. Surface ozone over southern Africa: synthesis of monitoring results during the cross border air pollution impact assessment project. *Atmospheric Environment* 38**:**6139-6147.

Zunckel, M, Cairncross, E, Marx, E, Singh, V & Reddy,V. 2004b. A dynamic air pollution prediction system for cape town, South Africa. *Transaction of the Wessex Institute*.